ANNUAL REVIEWS

Annual Review of Nuclear and Particle Science

The Search for Feebly Interacting Particles

Gaia Lanfranchi,[1] Maxim Pospelov,[2] and Philip Schuster[3]

[1]Laboratori Nazionali di Frascati, Istituto Nazionale di Fisica Nucleare, 00044 Frascati, Italy; email: Gaia.Lanfranchi@lnf.infn.it

[2]School of Physics & Astronomy and William I. Fine Theoretical Physics Institute, University of Minnesota, Minneapolis, Minnesota 55455, USA

[3]SLAC National Accelerator Laboratory, Menlo Park, California 94025, USA

Annu. Rev. Nucl. Part. Sci. 2021. 71:279–313

The *Annual Review of Nuclear and Particle Science* is online at nucl.annualreviews.org

https://doi.org/10.1146/annurev-nucl-102419-055056

Keywords

dark sectors, dark matter, beyond the Standard Model, feebly interacting particles

Abstract

At the dawn of a new decade, particle physics faces the challenge of explaining the mystery of dark matter, the origin of matter over antimatter in the Universe, the apparent fine-tuning of the electroweak scale, and many other aspects of fundamental physics. Perhaps the most striking frontier to emerge in the search for answers involves New Physics at mass scales comparable to that of familiar matter—below the GeV scale but with very feeble interaction strength. New theoretical ideas to address dark matter and other fundamental questions predict such feebly interacting particles (FIPs) at these scales, and existing data may even provide hints of this possibility. Emboldened by the lessons of the LHC, a vibrant experimental program to discover such physics is underway, guided by a systematic theoretical approach that is firmly grounded in the underlying principles of the Standard Model. We give an overview of these efforts, their motivations, and the decadal goals that animate the community involved in the search for FIPs, and we focus in particular on accelerator-based experiments.

Contents

1. INTRODUCTION

Feebly interacting particles (FIPs) have a notable history in fundamental physics. Indeed, weak interaction phenomena provided physics with an early example of a FIP in the form of a neutrino, and more recently dark matter (DM) has suggested the existence of additional types of FIPs. In addition to their empirical role, FIPs have been a common element of our most popular theoretical ideas to extend the Standard Model (SM), such as supersymmetry, and various low-energy limits of string theory. Even as particle physicists come to terms with null results from the LHC, which constrain New Physics (with sizable SM coupling) up to multi-TeV mass scales, many remaining theoretical ideas continue to predict FIPs in compelling ways. For example, FIPs provide excellent thermal DM candidates to extend the weakly interacting massive particle (WIMP) paradigm. The origin of neutrino masses and the matter–antimatter asymmetry in the Universe are easily explained in extensions of the SM with FIPs. The simplest theories to explain the origin of *CP* symmetry in strong interactions predict FIPs, and ideas to address the electroweak (EW) hierarchy problem and the origin of cosmological inflation also predict FIPs. Given their prevalence in theoretical approaches to extending the SM, and empirical evidence for their existence, interest in FIPs has grown steadily over time. Such interest has only accelerated in recent years, spurred on by anomalies in astrophysical data, precision SM measurements, and the profound lessons of the LHC.

Until a decade ago, most searches for FIPs were focused on EW mass scales, in large part because they were expected as part of a broader range of New Physics such as superpartners or extra dimensions. However, the bias toward these scales has eroded steadily because of LHC null

results and the growing recognition that FIPs can address SM puzzles over a wider mass range that extends well below the GeV scale. In fact, the degree to which FIPs were poorly constrained below the GeV scale caught physicists by surprise in many ways. Whereas below the MeV scale, stellar and cosmological data constrain FIP couplings to be much smaller than the couplings of weak forces, in the MeV–GeV range certain FIPs can interact more strongly than weak forces and still be compatible with existing data. This fact is all the more striking given that stable SM matter resides in this MeV–GeV range, and given how important these scales are to Big Bang nucleosynthesis (BBN), the QCD phase transition, and other aspects of the early Universe. These combined realizations spawned the development of a new generation of experiments over the past decade, which has now grown to include fixed-target and collider accelerators of all varieties, direct and indirect detection experiments, and precision measurements of SM parameters.

This review aims to summarize the current state of FIP physics (often called dark sector physics); we focus on the relatively unexplored MeV–GeV mass range and give special attention to accelerator-based experiments. Within this scope, our goals are to introduce particle physicists and astrophysicists to the essential motivations for FIPs, describe the most influential experimental techniques, and explain the compelling scientific milestones that energize the field as a whole. We also highlight the interconnections and synergy among different experimental techniques (such as accelerators and DM direct detection) as well as astrophysics and cosmology.

As described in Section 2, much of the phenomenology relevant to FIP searches can be understood from basic principles of quantum field theory and symmetry, which powerfully constrain the way new (SM neutral) physics can interact with SM matter. Historically, this led to the birth of the so-called portal formalism and the use of simple models to explore FIP phenomenology; it was assumed that more complex models aimed at addressing broader SM puzzles would inevitably be covered by this approach. This expectation has been borne out in recent years as more detailed models to address DM, the hierarchy problem, neutrino masses, and other puzzles have provided specific implementations of various simple models and have provided clues to help prioritize regions of parameter space that deserve special experimental attention. These studies have also brought into sharp focus a number of important scientific milestones, which we comment on throughout the review. Most of these milestones have focused on New Physics mass scales at or below the weak scale—in the same mass range as that of familiar matter and in the MeV–GeV range in particular.

As described in Sections 3–5, the experimental program that has emerged to pursue FIP science is diverse, and the interest in this field is reflected in many recent community planning documents, such as the Cosmic Frontier (1) and Intensity Frontier (2) reports of the 2013 Snowmass process, the dark sector community report (3), the US Cosmic Visions report (4), the LHC long-lived particles community white paper (5), the Physics Beyond Colliders BSM report (6), the white paper on new opportunities for next-generation neutrino experiments (7), and the *Physics Briefing Book* of the European Strategy for Particle Physics (8). Searches for FIPs at accelerator-based experiments in particular have triggered tremendous activity and are currently being performed at almost all the existing collider experiments and facilities, including the ATLAS, Belle II, CMS, and LHCb experiments at colliders and the HPS, MiniBooNE, NA62, NA64, and Super-Kamiokande experiments at extracted beam lines. Moreover, many new initiatives to cover important parameter space have emerged at CERN [CODEX-b (9), FASER (10, 11), MATHUSLA (12, 13), NA62 in dump mode (14), SHiP (15)], at SLAC [LDMX (16)], at FNAL [DarkQuest (17), DUNE Near Detector (18), M3 (19)], at MESA [DarkMESA (20)], at LNF [PADME (21)], at Jefferson Lab [BDX (22)], and at other laboratories. On a longer timescale, future high-energy electron and proton colliders will be able to explore higher mass ranges in a fully complementary way with respect to low-energy searches.

To fully explore the types of sub-GeV FIPs (or dark sectors) motivated by DM, the strong *CP* problem, and other mysteries of the SM, a healthy diversity of small- to medium-scale experiments operating at several facilities and employing a range of techniques will be required. Deriving meaningful scientific conclusions from these varied studies will require extensive collaboration and cross-fertilization across different communities (some such collaboration has already started in recent community planning initiatives). This is particularly true for sub-GeV DM searches; these efforts include searches in underground detectors via scattering of DM off nuclei or atoms (direct detection); observation of cosmic rays, γ-rays, and neutrinos produced by annihilation of DM in the cosmos (indirect detection); and searches for missing energy, momentum, and/or mass signals at accelerator-based experiments.

To help guide experimental efforts underway, the community should strive to use a common theoretical framework for FIPs and dark sectors that includes a representative set of minimal models built on clear theoretical principles of effective field theories. Adopting such a systematic approach will allow the community to combine and compare different experimental results. This is necessary to identify promising, still-uncovered regions of parameter space to guide future proposals and efforts and is also crucial for testing possible explanations in the case of positive signals.

In Section 6, we comment in some detail on recent scientific achievements that have resulted from FIP searches during the past 10 years, and we highlight next steps and milestones on which the field is currently focused. Some of these milestones are also called out in recent community prioritization efforts, such as the US Department of Energy's Basic Research Needs Workshop report (23) and the *Physics Briefing Book* of the European Strategy for Particle Physics (8).

2. MOTIVATIONS AND THEORETICAL FRAMEWORK

FIPs are any new (massive or massless) particles coupled to SM particles via extremely small couplings. The small strength of these couplings can be due to the presence of an approximate symmetry that is only slightly broken and/or to the presence of a large mass hierarchy between particles. FIPs are neutral under the SM gauge interactions, although a small weak neutral charge is possible. FIPs are fully complementary to New Physics with sizable couplings at the TeV scale explored (directly or indirectly) by the LHC experiments. Minimal models based on effective field theory have historically provided much of the guidance for exploring FIPs below the GeV scale, which we explain in Section 2.2.1. But first, we summarize the motivations for FIPs in the context of more general motivations for New Physics beyond the SM.

2.1. Motivations

There are many models of FIPs that include additional New Physics at higher mass scales, mostly driven by attempts to solve the Higgs hierarchy problem, such as MSSM with *R*-parity violation, split supersymmetry, and neutral naturalness (for a representative set of ideas, see, e.g., 24–28). While some of these ideas have certain merits, no undisputable top-down approach has emerged, and therefore in exploring the potential of FIPs as a solution to open problems in particle physics and cosmology, we prefer to adopt a phenomenological viewpoint, which is reflected in our summary below.

2.1.1. The electroweak hierarchy and strong *CP* puzzles. The incredible success of the SM in describing the vast majority of observable phenomena in nature comes hand-in-hand with the SM appearing fine-tuned in striking ways. One of the most puzzling aspects of the SM is the vast

hierarchy between the mass scale governing the strength of the gravitational force, $M_{\rm Planck}$, and the EW scale m_H : $m_H/M_{\rm Planck} \propto 10^{-17}$. The fact that the Higgs particle has so far not shown any experimental signs of compositeness suggests that the associated quantum field is susceptible to quantum corrections that would drive its mass toward the highest known scale of New Physics, which is presumably near $M_{\rm Planck}$. The vast separation between the observed Higgs mass and $M_{\rm Planck}$ therefore appears rather unnatural from a theoretical point of view.

Several theories try to address this issue by constructing specific mechanisms for cancellations of large quantum corrections to the Higgs mass (e.g., supersymmetry). Nevertheless, it is possible that some other selection mechanisms are at play that explore different alternatives. These include a much lower cutoff for the gravitational interactions [such as in theories with large extra dimensions (29)], leading to Kaluza–Klein copies of tensor and scalar gravitons—which in essence signifies the emergence of large numbers of extremely weakly coupled FIPs below the EW scale. Some other theories posit neutral naturalness (27, 28), which implies some type of discrete symmetry that entails the existence of light particles in the "approximately mirror" sector with extremely small couplings to the SM. Finally, it is conceivable that the Higgs mass was driven to its current value by some type of adjustment mechanism that exploits light scalar fields whose evolution drives the Higgs mass to today's value (30).

In many of these scenarios, the mechanism responsible for resolving the EW hierarchy problem implies that FIP states S couple to the Higgs boson in a manner described as follows:

$$(H^\dagger H) \times m_H^2 \longrightarrow (H^\dagger H) \times (m_H^2 + c_1 S + c_2 S^2 + ...). \qquad 1.$$

Such scenarios illustrate how models of New Physics can realize FIPs coupled via the Higgs portal (31, 32).

Another puzzling aspect of the SM is the extreme smallness of the parameter $\theta_{\rm QCD}$ that appears in front of gluon pseudoscalar density, $\theta_{\rm QCD} G^a_{\mu\nu} \tilde{G}^a_{\mu\nu}$, which manifests itself in a number of nonperturbative phenomena. Chief among these are effects linear in $\theta_{\rm QCD}$ that break *CP* symmetry and induce large (compared with experimental limits) electric dipole moments of the neutron and heavy atoms (33). A FIP-type solution to this problem was found many years ago (34–36). Promoting θ to a new dynamical field, the axion (perhaps a Goldstone remnant of some additional global Peccei–Quinn symmetry), we have the following:

$$\theta_{\rm QCD} G^a_{\mu\nu} \tilde{G}^a_{\mu\nu} \longrightarrow \left(\theta_{\rm QCD} + \frac{a}{f_a}\right) G^a_{\mu\nu} \tilde{G}^a_{\mu\nu}. \qquad 2.$$

Nonperturbative effects generate the new mass term that has $m_q \Lambda^3_{\rm QCD} \left(\theta_{\rm QCD} + \frac{a}{f_a}\right)^2$ dependence, which ensures that the minimum of the potential restores *CP* invariance of strong interactions. While original models had put f_a close to the EW scale ($f_a \sim v$), it was later realized that the range for it is much larger—a vast landscape for the QCD axion mass and coupling. Moreover, enlarging the number of similarly generated axion-like particles (ALPs) or axions and allowing for new m_a-generating mechanisms generalizes the QCD axion to a family of ALPs.

Finally, the gauge structure of the SM—the celebrated $SU(3) \times SU(2) \times U(1)$ group product—and the representations of SM matter fields are very suggestive of a unified gauge structure that in turn can have more low-energy remnants than the SM gauge group. Specifically, one may expect the following:

$$\begin{aligned} &[SU(3) \times SU(2) \times U(1)]_{\rm SM} \longrightarrow \text{GUT gauge group} \\ &\longrightarrow [SU(3) \times SU(2) \times U(1)]_{\rm SM} \times U(1)_X \times \ldots, \end{aligned} \qquad 3.$$

where an additional (or several additional) $U(1)_X$ may be gauging additional accidental symmetries of the SM, such as $B - L$, or be entirely new dark groups with very small couplings to the SM fields. If the mass scale for the additional $U(1)_X$ is small, the new gauge bosons and additional matter fields are also a motivated case for FIPs.

2.1.2. Neutrino oscillations imply a new matter sector. Precise measurements of neutrino flavor oscillations point to the existence of neutrino masses and a mismatch between weak and mass eigenstate bases. The nonzero neutrino mass dictates the existence of new states that participated in generating it. Among various neutrino mass generation mechanisms, the one that is based on a right-handed neutrino field N is the most economical and most natural, both for Dirac (D) and Majorana (M) neutrinos:

$$m_{\nu,\mathrm{D}}\bar{\nu}\nu \longrightarrow y_\nu \bar{N}\nu H + (\mathrm{h.c.}), \qquad 4.$$

$$m_{\nu,\mathrm{M}}\bar{\nu}\nu \longrightarrow (y_\nu)^2(\nu H)^c \times \frac{1}{m_N} \times (\nu H) + (\mathrm{h.c.}). \qquad 5.$$

The Dirac case is a clear example of a FIP, with a new field N sharing the same observable neutrino mass in the meV–eV range and implying a size of the Yukawa coupling as small as 10^{-13}. The Majorana case features a much heavier particle N, which we would refer to as a heavy neutral lepton (HNL); m_N^{-1} in the mass generation mechanism (also known as the seesaw mechanism) is the propagator of the HNL, $\langle N\bar{N}\rangle$. The possible mass range for the m_N is vast, and moreover, the seesaw scaling (37) $m_\nu \propto y_\nu^2 v^2 m_N^{-1}$ does not necessarily have to hold given the existence of multiple generations of HNLs and hidden symmetries among mass and Yukawa parameters.

It is intriguing that the Majorana mass term for HNLs breaks the lepton number by two units, and together with $B + L$ breaking provided by the nonperturbative EW effects at high temperatures, HNLs offer an attractive path to a dynamical generation of matter–antimatter asymmetry (38, 39). This scenario, known as leptogenesis, was shown to be viable both with heavy states and with HNLs below the EW scale (40), in which case they become perhaps the most motivated example of light fermionic FIPs.

2.1.3. Cosmology and astrophysics require New Physics. While so far we have discussed subtle observational effects [neutrino flavor oscillations, (non)conservation of *CP* invariance in strong interactions] and theoretical problems of the SM, the most urgent evidence for New Physics can be found in data from cosmology and astrophysics. The scientific revolution in cosmology over the past 25 years has brought certainty, and sometimes extreme precision, to our knowledge of the history and composition of the Universe. The 100% asymmetry between matter and antimatter, the necessity to generate the observable matter fluctuation spectrum, and above all the dominance of the dark sector energy density over "ordinary" matter all point to New Physics beyond the SM.

The DM—which is known to be cold and, to a certain extent, collisionless—had to be in existence prior to recombination. We know its abundance rather well, $\Omega_{\mathrm{DM}} \simeq 0.27$, which exceeds the abundance of atoms by a factor of 5.4. Other than that, its origin is a complete mystery apart from the knowledge that it is not composed of any known SM particles. It is very likely that remnants of the hot Big Bang account for the DM abundance. One can point to several generic classes of theoretical ideas, each with its own merit, that provide a consistent history for DM's creation, in which FIPs play an important role.

2.1.3.1. Freeze-out dark matter/weakly interacting massive particles. Even very small couplings of DM to SM particles can lead to efficient thermalization in the early Universe.

Subsequent expansion and cooling lead to the depletion of the DM energy density via, for instance, DM + DM → SM annihilation processes. In this case, the observed abundance of DM is set almost exclusively by the annihilation cross section. A thermally averaged $\langle \sigma v \rangle$ cross section, $\langle \sigma v \rangle = (2 - 4) \times 10^{-26}$ cm^3 s^{-1} $\simeq$ 1 pb $\times$ c, leads to a relic freeze-out abundance of stable DM particles that matches the observed DM fraction of the total average energy density in the Universe.

The canonical example of a minimal SM extension that realizes this scenario involves a heavy particle with a mass between 0.1 and 1 TeV interacting through the weak force (a WIMP). However, a thermal freeze-out origin is naturally valid even if the DM is at a lower mass: DM with any mass in the range of MeV to 100 TeV can achieve the correct relic abundance by annihilating directly into SM matter. Light (i.e., MeV–GeV range) WIMPs would be overproduced in the early Universe unless they were accompanied by an additional SM neutral mediator to enhance their annihilation rate (41–46). These dark sector mediators could be light, long-lived, vector or scalar FIPs that do not carry electromagnetic charge. This simple possibility that DM is a stable particle that interacts via FIPs (sometimes referred to as dark sector DM) is one of the most predictive motivations underlying experimental searches for FIPs.

2.1.3.2. Freeze-in dark matter. What if the DM interaction with the SM is so weak that full thermalization in the early Universe never occurs, while the initial abundance of such particles is negligible? The DM (e.g., an HNL particle) may be generated via SM → DM or SM → DM + DM processes. The requirement of being sufficiently cold typically restricts masses of such particles above $m_{\rm DM} \sim$ keV, while the size of couplings preventing thermalization has to be exceedingly small [often $\mathcal{O}(10^{-10})$ and smaller].

2.1.3.3. Bosonic condensate dark matter. As is well known, bosonic particles can have huge occupation numbers that vastly exceed a naive thermal estimate $\propto T^3$ of their number densities. This is a nonthermal starting point for a whole class of DM models that include the QCD axion. In general, the mass scale for such DM candidates is almost arbitrary; the only real restriction is that their coupling to the SM must be small. Not surprisingly, this whole class of DM candidates relies on DM to be a FIP. Thus we see that all three main classes of DM ideas feature FIPs, and for the rest of this review we concentrate on freeze-out DM because the prospects for its discovery/exclusion in laboratory experiments are the greatest.

To conclude this short cosmological discussion, we note that despite a seemingly endless number of possibilities for the solutions of cosmological problems, there are also severe restrictions implied by observations and their comparisons with ΛCDM predictions. For example, the initial stages of structure formation, recombination, and cosmic microwave background (CMB) decoupling occurred in a quiet Universe in which the nonthermal injection of ionizing radiation was reduced to a minimum (below ∼0.01–0.1 eV per baryon). This puts severe pressure on light WIMP models, should they continue their residual annihilation with a pbn × c rate at late times. It is also well known that the cosmological expansion during the BBN and the CMB epochs appears to have been normal; there is no evidence for additional thermalized degrees of freedom. Taken at face value, the cosmological expansion disfavors light thermalized DM with a mass of a few MeV or less. These constraints help to narrow down the spectrum of viable FIP models to masses above the MeV scale (see, e.g., 47).

2.2. Theoretical Framework

In this section, we provide an overview of the theoretical framework commonly used to describe the phenomenology of FIPs. We start with a summary of a general effective field theory formalism

Table 1 The portal formalism

Portal	Coupling
Vector: dark photon (A')	$-\frac{\varepsilon}{2\cos\theta_W} F'_{\mu\nu} B^{\mu\nu}$
Scalar: dark Higgs (S)	$(\mu S + \lambda_{\rm HS} S^2) H^\dagger H$
Fermion: heavy neutral lepton (N)	$y_N L H N$
Pseudo-scalar: axion (a)	$\frac{a}{f_a} F_{\mu\nu}\tilde{F}^{\mu\nu}$, $\frac{a}{f_a} G_{i,\mu\nu}\tilde{G}_i^{\mu\nu}$, $\frac{\partial_\mu a}{f_a}\overline{\psi}\gamma^\mu\gamma^5\psi$

(i.e., portal formalism), followed by more detailed discussion of each of the major classes of FIP interactions with SM matter.

2.2.1. The portal formalism. To begin, consider new particles that do not carry electromagnetic, weak, or strong interaction charges. Such particles are often referred to as part of a hidden sector or dark sector. Let $O_{\rm SM}$ be an operator composed of SM fields and $O_{\rm DS}$ an operator composed of dark sector fields. The portal framework (see, e.g., 6, 31, 48, 49) refers to a systematic way to describe all such interactions between a dark sector and the SM by building an interaction Lagrangian out of the products of such operators:

$$\mathcal{L}_{\rm total} = \mathcal{L}_{\rm SM} + \mathcal{L}_{\rm DS} + \mathcal{L}_{\rm portal};\ \ \mathcal{L}_{\rm portal} = \sum O_{\rm SM} \times O_{\rm DS}, \qquad 6.$$

where the sum goes over a variety of possible operators and varying composition and dimension. Note that only the product of the operators must be a Lorentz scalar, while $O_{\rm SM}$ and $O_{\rm DS}$ can transform as, for instance, a spinor or Lorentz tensor. However, given the assumption of the SM neutrality of the dark sector, both types of operators separately must be complete gauge singlets, and this requirement places a powerful constraint on the types of interactions that are allowed.

As commonly defined, the minimal portals consist of the lowest canonical-dimension operators that mix new dark sector states with gauge-invariant (but not necessarily Lorentz-invariant) combinations of SM fields. Based on the general principles stated above, the collection of such portals is rather simple (see **Table 1**). Finally, while $\mathcal{L}_{\rm portal}$ has a minimal number of options, the dark sector Lagrangian itself can be far more complicated, and A', S, N, and a can connect, even at the renormalizable level, to completely new particles and fields.

In **Table 1**, $F'_{\mu\nu}$ stands for the field strength of a dark gauge group, which couples to the hypercharge field, $B^{\mu\nu}$; S is a new scalar singlet that couples to the Higgs doublet, H, with dimensionless and dimensional couplings, $\lambda_{\rm HS}$ and μ; and N is a new neutral fermion (or HNL) that couples to one of the left-handed doublets of the SM and the Higgs field with a Yukawa coupling, y_N. These three cases capture most UV-complete portal interactions, which are, as such, unsuppressed by any possible large (or very large) New Physics scale Λ. We discuss possible enlargement of this set in Section 2.3. These three interactions, which are neutral under all the SM symmetries, keep the EW sector of the SM completely intact. While many new operators can be written at the nonrenormalizable level, a particularly important example is provided by the axion (or axion-like) particle a that couples to gauge and fermion fields at dimension 5. This is described by the pseudoscalar portal, which is suppressed by $1/f_a$, where f_a is called the axion decay constant.

SM symmetries have a number of important built-in properties, such as minimal flavor violation (in which all flavor violation is associated only with the SM Yukawa matrices), minimal Higgs content, and separate perturbative conservation of lepton number and baryon number. The first two portals shown in **Table 1** fully preserve this minimal SM flavor structure, and therefore they are not constrained by, for instance, K-B meson mixing and/or charged lepton conservation. However, the HNL interactions do introduce new flavor dependence via y_N and/or the mass term for the HNLs themselves. This mass term—if Majorana—will also effectively break the lepton

number by two units, making it a unique feature of this portal. Finally, the axion interaction with the SM fermions can source flavor violation in both the lepton and quark sectors. A more detailed description of the four portals is reported in the subsections below.

2.2.2. Vector portal. A considerable amount of the theoretical and experimental attention of recent years has focused on the vector (i.e., dark photon) portal, and there is a distinct possibility that the new matter fields charged under the associated $U(1)_{A'}$ provide a viable thermal DM candidate. The minimal dark sector Lagrangian can be written as follows:

$$\mathcal{L} = -\frac{1}{4}F'_{\mu\nu}F'_{\mu\nu} - \frac{\varepsilon}{2}F'_{\mu\nu}F'_{\mu\nu} + A'_\mu J^{\rm dark}_\mu + \mathcal{L}_{\rm mass} + ..., \qquad 7.$$

where the dark current is given by the interaction of the A' with either new fermions or new scalars: $J^{\rm dark}_\mu = g_{\rm D}\bar{\chi}\gamma_\mu\chi$; $ig_{\rm D}(\chi^*\partial_\mu\chi - \chi\partial_\mu\chi^*)$. The mass Lagrangian may include $\frac{1}{2}m^2_{A'}(A'_\mu)^2$, $m_\chi\bar{\chi}\chi$, and $m^2_\chi\chi^*\chi$ terms as well as interactions that could introduce spontaneous $U(1)_{A'}$ breaking (i.e., dark Higgs mechanism) and/or mass splitting of χ matter fields. The exchange by the mixed photon–dark photon propagator creates an interaction between the SM electromagnetic current and dark currents,

$$V_{\rm int}(q) = J^{\rm EM}_\mu \frac{\varepsilon}{q^2 - m^2_{A'}} J^{\rm dark}_\mu, \qquad 8.$$

which is suppressed by the small kinetic mixing parameter ε. We note that taking an $m_{A'} \to 0$ limit corresponds to giving χ particles an EM millicharge, $Q_\chi = g_{\rm D} \times \varepsilon$. In the above, we have neglected the induced coupling of the dark current to the SM weak current because it is additionally suppressed by $(m_{A'}/m_Z)^2$ and therefore can often be omitted at low energies.

The set of minimal models connected to the vector portal is theoretically appealing in several respects. The smallness of ε can result from radiative effects where loops of matter charged under the SM gauge groups and $U(1)_{A'}$ will naturally generate a nonzero mixing angle ε, while $g_{\rm D}$ is not required to be small. Depending on the details of the loop-level UV physics, ε could vary in a wide range (e.g., 10^{-15} to 10^{-1}), though the naive one-loop estimate gives $\varepsilon \sim 10^{-4}$ to 10^{-2}, and GUT-inspired supersymmetric models tend to give $\varepsilon \sim 10^{-6}$ to 10^{-3} (50, 51).

Perhaps the greatest appeal of this class of models is that they easily accommodate a minimally coupled WIMP-like DM candidate. The interaction described in Equation 8 allows for the annihilation of two dark particles to a pair of charged SM fermions, $\chi\bar{\chi} \to \psi_{\rm SM}\bar{\psi}_{\rm SM}$, or more generically to all combinations of the SM particles that can be created from the vacuum by the EM current. The CMB bounds on late energy injection (52) are easily evaded if the annihilation occurs in the P-wave (such as for a scalar or Majorana χ) or if the mass splitting in the $\chi\bar{\chi}$ system cuts off the late time annihilation (53).

The frequently analyzed parameter space for this model consists of $(\alpha_D, \varepsilon, m_{A'}, m_\chi)$, where $\alpha_D = g^2_D/4\pi$ is the dark coupling between DM and the vector mediator. Moreover, for achieving the correct DM abundance, a specific combination y of these parameters is introduced (53):

$$y = \alpha_D\varepsilon^2\alpha\left(\frac{m_\chi}{m_{A'}}\right)^4, \qquad 9.$$

which, away from the $2m_\chi \simeq m_{A'}$ resonance, more or less directly determines the annihilation rate, $\langle\sigma v\rangle \sim y \times m_\chi^{-2}$, and hence the final relic density. Tuning this rate to the one required to achieve the observed DM abundance defines a preferred range (i.e., thermal target) on the (m_χ, y) parameter space.

It is clear that the Lagrangian shown in Equation 7 and the interaction shown in Equation 8 provide a basis for experimental studies of FIPs coupled via the vector portal. Production of the A'

(or DM particle–antiparticle pairs $\chi\bar{\chi}$) with subsequent decay to SM or dark particles represents one of many distinct possibilities for exploration of the vector portal in a wide variety of ongoing and planned experiments.

2.2.3. Scalar portal. The discovery of the Higgs boson h has prompted investigation of the so-called scalar or Higgs portal that couples the dark sector to the Higgs boson via the bilinear $H^\dagger H$ operator of the SM. The minimal scalar portal model (see, e.g., 31, 32, 43) operates with one extra singlet field S and two types of dimensional and dimensionless couplings (μ and $\lambda_{\rm HS}$, respectively):

$$\mathcal{L}_{\rm scalar} = \mathcal{L}_{\rm SM} + \mathcal{L}_{\rm DS} - (\mu S + \lambda_{\rm HS} S^2) H^\dagger H. \quad 10.$$

This model can be easily generalized to multiple scalars. Intriguingly, the μ-proportional portal belongs to the class of superrenormalizable operators and is unique in that respect among all portal couplings that we consider.

The dark sector Lagrangian may include the interaction with DM χ, $\mathcal{L}_{\rm DS} = S\chi\overline{\chi}... + ...$ Most viable DM models in the sub-EW-scale range imply $m_\chi > m_S$ and hence a secluded annihilation (43) $\chi\chi \to SS$ via a t-channel, P-wave transition.

At low energy, the Higgs field can be substituted for $H = (v + h)/\sqrt{2}$, where $v = 246$ GeV is the EW vacuum expectation value and h is the field corresponding to the physical 125-GeV Higgs boson. The nonzero μ leads to the mixing of h and S states. In the limit of small mixing it can be written as follows:

$$\theta = \frac{\mu v}{m_h^2 - m_S^2}.$$

Hence, the hidden scalar couples to SM fermions and vector bosons as an SM Higgs but with a strength reduced by a factor of $\sin\theta$, where θ is the mixing angle between the two sectors.

The coupling constant $\lambda_{\rm HS}$ leads to the coupling of h to a pair of S particles, $\lambda_{\rm HS} S^2$. It can lead to pair production of S but cannot induce its decay. Therefore, in this case the scalar singlet does not mix with the Higgs as in the case of an exact Z_2 symmetry. By itself, such a scalar with the Z_2 symmetry was often considered as a candidate for DM (32). However, the experimentally observed Higgs particle with no detectable invisible decay channel, together with new advances in direct detection, relegates the surviving mass range to a multi-TeV region.

An important property of the scalar portal—and the crucial difference with the vector portal—is in the phenomenology of flavor-changing neutral currents (FCNCs). While both portals preserve flavor at tree level, the t-W loop-induced FCNC amplitudes for $b \to s, d$ and $s \to d$ transitions behave in a markedly different way (54). Because of conservation of the EM current, the dark photon penguin amplitudes are effectively suppressed (aside from the usual loop factors and CKM matrix elements) by $G_{\rm F} m^2_{\rm meson}$. In the scalar portal case there is no current conservation, and an analogous combination scales as $G_{\rm F} m_t^2$, leading to an enormous enhancement factor. In practical terms, it means that the production of light FIPs via scalar portal will occur via K and B mesons. Thus, experiments with copious flavored particle production (e.g., high-luminosity e^+e^- B factories, kaon and neutrino beam experiments, the LHC and hadronic beam dumps at high enough energy) are particularly suited to exploring the scalar portal in the low mass range.

In addition to the case of very small μ, $\lambda_{\rm HS}$ parameters, we note that larger values for these couplings may also bear interesting consequences. The existence of a new scalar field tends to change the nature of the EW phase transition, making it first-order and reopening the door for the EW baryogenesis (38, 55, 56) if additional new sources of CP breaking are added into the theory.

2.2.4. Fermion (neutrino) portal. The neutrino portal operates with one or several HNL states. The general form of the neutrino portal can be written as follows:

$$\mathcal{L}_{\text{fermion}} = \mathcal{L}_{\text{SM}} + \mathcal{L}_{\text{DS}} + \sum F_{\alpha I}(\overline{L}_\alpha H)N_I, \qquad 11.$$

where the summation goes over the flavor of lepton doublets L_α and the number of available HNLs, N_I. The $F_{\alpha I}$ are the corresponding Yukawa couplings. The dark sector Lagrangian should include the mass terms for HNLs, which can be both Majorana or Dirac type. Setting the Higgs field to its vacuum expectation value and diagonalizing mass terms for neutral fermions, one arrives at $\nu_i N_J$ mixing, which is usually parameterized by a matrix called U. Therefore, to obtain interactions of HNLs, one can replace ν_α with $\sum_I U_{\alpha I} N_I$ inside the SM interaction terms. In the minimal HNL models, both the production and decay of an HNL are controlled by the U matrix elements. While it would be difficult to imagine a case where an HNL would couple to only one linear combination (or a single flavor) of charged leptons, it is nevertheless customary to assume a single flavor dominance as a way of comparing experimental reach.

The emergence of Ns in weak charged and neutral currents immediately signals that the best way of producing and detecting the HNLs is via the decays of on-shell or off-shell W and Z bosons. Therefore, similar to the case of the scalar portal, the LHC experiments, various flavor experiments, neutrino beam experiments, and hadronic beam dumps are among the most promising venues in searches for HNLs. At the same time, the number of currently planned experiments that could deliver competitive sensitivity to (m_N, U_α) parameter space remains comparatively small.

The cosmology and astrophysics of HNLs are very diverse, and we will not cover them in any substantial detail in this review; we note primarily that HNLs are a promising DM candidate. If, for example, all $U_{\alpha I}$ leading to HNLs in the keV–MeV mass range are sufficiently small, they lead to an effective cosmological meta-stability. In that case, $\nu_{\text{SM}} \rightarrow$ HNL oscillations in the early Universe may lead to the correct cosmological abundance via freeze-in (57). However, the latest constraints on fluxes of X-rays that result from $\text{HNL}_{\text{DM}} \rightarrow \gamma\nu_{\text{SM}}$ decays seem to indicate that the most straightforward mechanism for populating the DM is already excluded. Variants of this model—for instance, with extra dark states interacting with HNLs—may solve this underabundance problem.

2.2.5. Pseudoscalar portal. Taking a single pseudoscalar field a, one can write a set of its couplings to photons, gluons, and other fields of the SM. In principle, the set of possible couplings is very large, and in this review we consider only the flavor-diagonal subset:

$$\mathcal{L}_{\text{axion}} = \mathcal{L}_{\text{SM}} + \mathcal{L}_{\text{DS}} + \frac{a}{4f_\gamma}F_{\mu\nu}\tilde{F}_{\mu\nu} + \frac{a}{4f_G}\text{Tr}G_{\mu\nu}\tilde{G}_{\mu\nu} + \frac{\partial_\mu a}{f_l}\sum_\alpha \bar{l}_\alpha\gamma_\mu\gamma_5 l_\alpha + \frac{\partial_\mu a}{f_q}\sum_\beta \bar{q}_\beta\gamma_\mu\gamma_5 q_\beta. \qquad 12.$$

Because of the derivative nature of all perturbative interactions in Equation 12, there is no direct feedback from quantum-loop SM particles to the mass of a. (As mentioned above, only $G\tilde{G}$ coupling can participate in contributing to m_a at a nonperturbative level.) However, the power counting of divergencies in the perturbative renormalization of the kinetic term $(\partial_\mu a)^2$ shows quadratic sensitivity to UV scales $(\sim \Lambda^2 f_a^{-2})$, signaling the need for UV completion. One can imagine that the dark sector Lagrangian may contain a new UV sector, the so-called the Peccei–Quinn sector, with an approximate global symmetry, providing the required completion. This is fundamentally different from vector, scalar, and neutrino portals that do not require external UV completion, and it requires in all the calculations the introduction of a cutoff scale. However, the laboratory reach to a often has very weak dependence on details of UV completion.

The cosmology of axions and ALPs is quite sensitive to their masses and coupling constants, and because of the higher-dimensional nature of their coupling, it may be sensitive to the initial

conditions in the early Universe, such as the reheat temperature at the end of inflation. It is also important whether the Peccei–Quinn symmetry itself remained unbroken during inflation. Stringent limits on QCD axions can be derived from stellar energy loss arguments. Combined with estimates of cosmological abundance of axions starting from generic (i.e., not tuned) initial conditions, an "expectation band" can be estimated for the mass-coupling relation that would give QCD axions the total energy density comparable to that of the observed DM, while astrophysical constraints typically favor a sub-eV mass range. A more generic version—an ALP—can constitute DM for a much larger range of masses and couplings.

Axion and ALP searches must span a wide range of ALP masses, especially if the mass range is extended to be above ∼1 MeV. They can be directly produced in colliders or beam dump experiments or can result from the FCNC decays of flavored mesons. Similar to the Higgs portal case, the generic axion coupling is not conserved, and sizable loop-induced FCNC amplitudes result. Experimental attention to ALPs above the MeV scale is relatively recent, and many new experimental and theoretical results are expected soon.

2.3. Extending Minimal Portals

The framework reviewed in the sections above represents a guiding principle and captures many important phenomena in FIP physics, yet it can be extended. Below, we give a brief account of some of these extensions.

- Gravity portal: All FIPs are guaranteed to have a minimal gravitational coupling, but the bosonic fields can also directly couple to the graviton's kinetic term, as in theories of large extra dimensions (29).
- Gauging of the SM accidental symmetries: Besides the dark photon [which can be rewritten as a new gauge field coupled to hypercharge (58)], there exist examples of other well-motivated $U(1)$ extensions of the SM, such as $U(1)_{B-L}$ gauge symmetries that arise in GUTs, and so-called left–right extensions of the SM gauge group (59).
- Flavor nonuniversal extensions: Gauging individual flavor numbers in the lepton sector, such as $L_\mu - L_\tau$, does not lead to any immediate flavor problems and allows the corresponding gauge boson mass to be in the sub-GeV range, giving, for instance, a potentially sizable contribution to muon $g-2$.
- Extensions built with $d \geq 6$ operators: Light FIPs may interact with the SM by way of heavy mediators. Integrating these mediators out of the theory results in interactions that typically have dimensions $\geq$6, suppressed by powers of the mediator mass scale. The possibility of accessing FIPs via higher-dimensional operators has come into focus relatively recently in connection with, for instance, hidden valley (60) and neutral naturalness ideas (27, 28).
- Neutron portal: New FIP particles χ may be coupled to neutrons (or more generically to electrically neutral baryons) via $\bar{n}\chi$ + h.c. mixing terms, leading to nontrivial phenomenological consequences for n-χ oscillation and/or n decay.

The portal framework provides a structured approach to the physics of FIPs and harmonizes a large multitude of experimental searches. Yet this formalism should be considered a gateway toward more fundamental and complete models, the structure of which can be important to consider once convincing FIP signals show up in experiments. In the following sections, we focus mostly on results or projections of accelerator-based experiments obtained using the minimal portal framework.

2.4. Synergy and Complementarity with Direct Dark Matter Detection Experiments, Astroparticles, and Cosmology

Rapid developments in DM direct detection have brought gains in sensitivity to WIMP cross sections and, importantly for our FIP discussion, have lowered detection thresholds for some experiments. Consequently, some of the DM models discussed in connection with FIP portals may be probed in direct detection.

To make this connection well defined, the spin choice and mass terms of the DM model must be specified. For example, in the absence of any $U(1)_{A'}$-breaking mass terms, complex scalar DM with a dark photon mediator (see Section 2.2.2) predicts the scattering on electrons to be ($m_e \ll m_\chi$)

$$\sigma_{\chi e} = \frac{16\pi\alpha\alpha_D\varepsilon^2 m_e^2}{m_{A'}^4} = \frac{16\pi\alpha m_e^2}{m_\chi^4} \times y \simeq 3.7 \times 10^{-27}\,\mathrm{cm}^2 \times (10\,\mathrm{MeV}/m_\chi)^4 \times y, \qquad 13.$$

with a similar formula for the scattering on nuclei. Here y is the same yield parameter that largely controls the abundance (see Equation 9). Consequently, low-threshold direct detection experiments probing DM-nucleus scattering can rule out significant fractions of parameter space for this model (e.g., $m_\chi > 400$ MeV is disfavored by CRESST; see 61 and discussion in Section 5.1.1), while future planned DM-electron experiments have yet to achieve the levels of sensitivity relevant for sub-GeV freeze-out DM.

It is important to stress the underlying physical complementarity between direct detection and accelerator probes, especially when comparisons are made. Ultimately, direct detection probes DM deep in the nonrelativistic limit, whereas accelerator experiments probe DM interactions in the relativistic limit, and this distinction has profound consequences on the phenomenology. For example, different choices of DM spin can lead to direct detection rates suppressed by multiple powers of DM halo velocity $v \sim 10^{-3}$ among different models, whereas accelerator rates are only mildly affected by changing the spin because production occurs near $v \sim 1$. Additionally, direct detection rates are extremely sensitive to even small perturbations of the DM mass terms that are potentially present in $\mathcal{L}_{\mathrm{mass}}$ in Equation 7. In particular, the $U(1)_{A'}$-breaking mass term $\Delta m^2\chi^2$ generates a mass splitting Δm between the real components of $\chi = 2^{-1/2}(\chi_1 + i\chi_2)$ that is easily larger than the kinetic energy of WIMPs today [$E_{\mathrm{kin}} \sim \frac{1}{2}m_\chi c^2(v_{\mathrm{SM}}/c)^2 \sim 10^{-5}\,\mathrm{eV} \times m_\chi/20\,\mathrm{MeV}$]. In this case, S-wave elastic direct detection scattering is completely quenched but has a negligible effect on the primordial abundance. Similar arguments apply to fermionic DM. Therefore, the direct detection program alone cannot be viewed as a universal substitute for the accelerator-derived probes of the vector portal DM models. Likewise, accelerator probes alone cannot verify that the particles produced are indeed cosmologically long-lived. Both types of experiments are crucially important.

As mentioned above, the early Universe puts serious restrictions on many variants of the portal models and carves out significant parts of the parameter space in what appears to be direct competition with accelerator-derived bounds. For example, HNLs at the scale of 100 MeV–GeV are partly excluded by the primordial nucleosynthesis (i.e., BBN). The production in the early Universe, even with initially absent HNLs, results in their substantial presence during the neutron–proton interconversion freeze-out. This typically limits the lifetimes of HNLs to a fraction of a second, resulting in tight limits on mixing angle versus mass. Similar considerations apply to the Higgs mixed scalar. Dark photons in the experimentally accessible mixing-angle range are typically too short-lived to be limited through BBN. However, if dark photons are supplied with WIMP-type DM, its annihilation to the electron–positron pairs is constrained. DM that is too light (i.e., below a few MeV) has an unmistakable signature of injecting more energy to the photon fluid, thus effectively reducing N_{eff}, a commonly used parameter to characterize neutrino energy density

relative to photons. For many other models, FIPs may lead to an increase in $N_{\rm eff}$—for example, in models of millicharged dark particles coupled to the SM via massless A'. In addition, as mentioned above, residual annihilation of DM during the recombination will lead to the discrepancy of the CMB angular anisotropy data with ΛCDM. This imposes strong restrictions on admissible WIMP models. However, declaring S-wave annihilating light WIMPs to be excluded would be an overreach. Indeed, the same mass splitting perturbations in $\mathcal{L}_{\rm mass}$ may leave freeze-out annihilation unchanged while significantly suppressing the annihilation at $z \sim 10^3$ and below, which is relevant for the CMB bounds. Again, one observes the complementarity of cosmological bounds to direct searches.

Finally, stellar energy loss and especially supernovae provide relevant bounds on light particles at the scale of a few MeV to 100 MeV. If too much energy is taken away from the exploding star, the energetics of the explosion changes, potentially affecting its development and degrading the neutrino signal observed from SN 1987A. As a result, similar to the beam dump studies, supernovae exclude certain regions of parameter space corresponding to sufficient production and relatively small absorption and rescattering of newly produced particles inside the star.

3. EXPERIMENTAL LANDSCAPE

Searches for FIPs at accelerator-based experiments have recently received significant attention in the experimental high-energy physics community because they offer an ideal way to search the well-motivated MeV–GeV mass range, as discussed in Section 2. Results from many past experiments have been reinterpreted within the portal formalism, new searches are being performed in many existing experiments at colliders and extracted beam lines, and new proposals have been presented at major laboratories worldwide. **Table 2** summarizes the main past, current, and future experiments aimed at detecting FIPs, the beam type, the collected or expected data set, the experimental technique used, and the main portals the experiments are sensitive to. More details are provided in the **Supplemental Appendix**.

Supplemental Material >

Accelerator experiments represent a unique tool to test models with light DM in the MeV–GeV range. The advantage of accelerator experiments is that the DM is produced in the relativistic regime in a controlled manner and at an energy scale similar to that which governs the annihilation and thermal decoupling of DM from the SM in the early Universe. This allows one to make predictions about the strength of accelerator DM signals based on the observed abundance of DM. Because the energy scales of thermal freeze-out and accelerator production are similar, these predictions tend to be fairly robust against variations of the underlying model that might severely affect nonrelativistic signals such as scattering in direct detection (see Section 2.4).

Beyond light DM, FIPs with very small SM couplings are naturally very long-lived particles compared with SM particles; this fact has motivated experiments with long decay volumes to detect FIP decays in visible final states. The presence of feeble couplings also means that these decays are very rare; hence, effective background rejection is paramount. For this reason, detectors need to have excellent tracking systems with the capability to precisely reconstruct displaced vertices and identify different species of hadrons and leptons for visible FIP decays. Another strategy is to precisely determine the kinematics of the events to constrain FIPs that are sufficiently long-lived to escape direct detection (as missing mass or via missing momentum techniques; see Sections 4.3 and 4.4).

In Section 4, we describe the most commonly used experimental techniques. Section 5 shows the multitude of results for FIP searches and projections for future experimental initiatives cast in the minimal portal framework, as discussed in Section 2.2.1.

Table 2 Main past, current, and future accelerator-based experiments sensitive to FIP searches

Experiment	Lab	Beam	Particle yield/$\mathcal{L}$	Technique	Portals
Past					
LSND (62)	LANL	p, 800 MeV	10^{23} pot	e^- recoil	V
E137 (63)	SLAC	e^-, 20 GeV	2×10^{20} (30 C)	Visible	V, P
E141 (64)	SLAC	e^-, 9 GeV	2×10^{15}	Visible	V, P
E774 (65)	FNAL	e^-, 275 GeV	2×10^{15}	Visible	V
NuCal (66, 67)	Serpukhov	p, 70 GeV	1.7×10^{18}	Visible	V, P
CHARM (68)	CERN	p, 400 GeV	2.4×10^{18}	Visible	V, S, P, F
MiniBooNE (69)	FNAL	p, 8 GeV	1.9×10^{20}	Recoil e, N	V
KLOE (70, 71)	LNF	e^+e^-, 1 GeV	Up to 1.7 fb^{-1}	Visible, invis.	V
NA48/2 (72)	CERN	π^0	2×10^7	$\not{M}$	V
Belle (73)	KEK	e^+e^-, 10.58 GeV	0.6–0.8 fb^{-1}	Visible	V, S, F
BaBar (74)	SLAC	e^+e^-, 10.58 GeV	514 fb^{-1}	Visible, invis.	V
Current					
ATLAS (75)	CERN	pp, 13–14 TeV	Up to 3 ab^{-1}	Visible, invis.	V, S, P, F
CMS (76)	CERN	pp, 13–14 TeV	Up to 3 ab^{-1}	Visible, invis.	V, S, P, F
LHCb (77)	LHC	pp, 13–14 TeV	Up to 300 fb^{-1}	Visible	V, S, P, F
Belle II (78)	KEK	e^+e^-, 11 GeV	Up to 50 ab^{-1}	Visible, invis.	V, S, P, F
BES III (79)	BEPC II	e^+e^-, 3.7 GeV	Up to 40 fb^{-1}	Invis.	V
NA62 (80)	CERN	K^+, 75 GeV	Up to 10^{13} K decays	Visible, invis.	V, S, P, F
NA64$_e^{++}$ (81)	CERN	e^-, 100 GeV	Up to 3×10^{12} eot/year	$\not{E}$, visible	V, P
HPS (82)	JLAB	e^-, 2–6 GeV	$\sim 10^{20}$ eot	Visible	V, P
APEX (83)	JLAB	e^+, 2.2 GeV	Up to 150 μA	Visible	V
MicroBooNE (84)	FNAL	p, 8 GeV	$\sim 10^{21}$ pot	Recoil Ar	V
Dark(Sea)Quest (85)	FNAL	p, 120 GeV	$10^{18} \rightarrow 10^{20}$	Visible	V, S, P, F
T2K-ND280 (86)	JPARC	p, 30 GeV	10^{21} pot	Visible	F
PADME (21)	LNF	e^+, 550 MeV	5×10^{12} e^+ot	Missing mass	V
PIENU (87)	TRIUMF	π^+, 75 MeV	10^7	Missing mass	F
Future/proposed					
SHiP (15)	CERN	p, 400 GeV	2×10^{20}/5 years	Visible, recoil	V, S, P, F
NA62-dump (14)	CERN	p, 400 GeV	$\sim 10^{18}$ pot	Visible	V, S, P, F
NA64$_\mu$ (88)	CERN	μ, 160 GeV	Up to 10^{13} mot/year	$\not{p}$	V
RedTop (89)	CERN	p, 1.8 and 3.5 GeV	Up to 10^{17} pot	Visible	S, P
DarkMESA (20)	Mainz	e^-, 155 MeV	150 μA	Visible	V
LDMX (16)	SLAC	e^-, 4 and 8 GeV	2×10^{16} eot	$\not{p}$, visible	V
SBND (90)	FNAL	p, 8 GeV	6×10^{20} pot	Recoil Ar	V
LBND (18)	FNAL	p, 120 GeV	$\sim 10^{21}$ pot	Recoil e, N	V, S, P, F
M^3 (19)	FNAL	μ, 15 GeV	10^{10} (10^{13}) mot	$\not{p}$	V
FASER 2 (91)	CERN	pp, 14 TeV	150 fb^{-1} $\rightarrow$ 3 ab^{-1}	Visible	V, S, P, F
CODEX-b (9)	CERN	pp, 14 TeV	300 fb^{-1}	Visible	V, S, P, F
MATHUSLA (12)	CERN	pp, 14 TeV	3 ab^{-1}	Visible	V, S, P, F
milliQan (92)	CERN	pp, 14 TeV	0.3–3 ab^{-1}	Visible	V
MoeDAL/MAPP (93)	CERN	pp, 14 TeV	30 fb^{-1}	Visible	F
BDX (94)	JLAB	e^-, 11 GeV	$\sim 10^{22}$	Recoil e	V, P
DarkLight (95)	JLAB	e^-, 100 MeV	5 mA	Visible	V
Mu3e (96)	PSI	29 GeV	$10^{18} \rightarrow 10^{20}$ μ/s	Visible	V

Abbreviations used in Portals column: V, vector; S, scalar; P, pseudoscalar; F, fermion.

4. EXPERIMENTAL TECHNIQUES

Searches for FIPs at accelerator-based experiments are performed with a large variety of beam lines and cover an impressive range of masses, from a few MeV to a few TeV. Many different experimental techniques are used. They depend on the characteristics of the available beam lines and detectors and can be categorized as discussed in the subsections below.

4.1. Detection of Visible Decays

HNLs, ALPs, and in general light DM mediators feebly coupled to SM particles can decay to visible final states with a probability that depends on the model and scenario. For example, if the mediators between SM and light DM particles have a mass less than twice the DM mass, once produced they can decay only to visible final states.

The detection of visible final states is a technique used in almost all existing experiments searching for FIPs, but it is used the most in experiments operating with proton beams (either beam dump or *pp* colliders) where the background is typically very large and the kinematics of the signal production process is often not known. Typical signatures are expected to show up as narrow resonances over an irreducible background. The use of this technique requires high-luminosity colliders or large fluxes of protons and/or electrons on a dump because the detectable rate of FIPs is proportional to the fourth power of the coupling involved, g^4, and is therefore very suppressed for very feeble couplings. Moreover, visible FIP decays to SM particles require long decay volumes followed by spectrometers with excellent tracking systems and particle identification capabilities to disentangle very long-lived and elusive signals from usually large backgrounds.

Existing or past experiments using this technique are (*a*) at e^+e^- colliders [Belle (73), BaBar (74), KLOE (70, 71), and Belle II (78)]; (*b*) at *pp* colliders [ATLAS (75), CMS (76), and LHCb (77)]; (*c*) at proton beam dumps [CHARM (68) at CERN]; and (*d*) at electron beam dumps [E137 (63) and E141 at SLAC (64), NA64$_e$ (97) at CERN, and HPS (82) and APEX (83) at Jefferson Lab]. Future proposals aiming to use this technique are (*a*) at the LHC [MATHUSLA (12, 13), FASER 2 (10, 11), CODEX-b (9), ANUBIS (98), and MoeDAL/MAPP (93)]; (*b*) at proton beam dumps [DarkQuest (or SeaQuest) (99) at FNAL; NA62 in dump mode (14) and SHiP (15) at CERN]; and (*c*) at e^+e^- colliders [BES III (79)].

4.2. Direct Detection of Light Dark Matter Scattering off the Detector Material

Light DM produced in reactions of electrons and/or protons with a dump can travel across the dump and be detected via scattering off the electrons and/or protons of the detector. This technique has the advantage of directly probing the DM production processes, but it requires a large proton and/or electron yield to compensate for the small scattering probability (see, e.g., Equation 13). Moreover, the signature is very similar to that produced by neutrino interactions, and this is a limiting factor for proton beam dump experiments unless it is possible to use a bunched beam and time-of-flight techniques. Of course, this is much less a concern for electron beam dump experiments. In both electron and proton beam dump experiments, large factors can be gained by considering secondary products in the shower (e.g., positrons annihilating with the electrons in the medium) as potential sources of light DM. Existing or past experiments using this technique include (*a*) proton beam dumps [LSND (62), MiniBooNE (69), and MicroBooNE (84) at FNAL] and (*b*) electron beam dumps [BDX (94) at Jefferson Lab]. Future experiments include SBND (90) and MPD (18) at FNAL.

4.3. Missing Momentum and Missing Energy Techniques

Very long-lived FIPs or FIPs decaying into light DM states can be detected in fixed-target reactions (e.g., $e^- Z \to e^- Z A'$, where A' is a dark photon) by measuring the missing momentum ($\not{p}$) or missing energy ($\not{E}$) carried away from the escaping invisible particle(s). As such, these techniques apply to a broad class of models.

The missing momentum technique exploits the change in the kinematics of a particle induced by crossing a target without being completely stopped, which can be measured by tracking systems upstream and downstream of the target. This technique will be used mostly by the proposed experiments LDMX (16) at SLAC, M^3 (19) at FNAL, and $NA64_\mu$ (88) at CERN. In the case of missing energy, the signal is instead a beam energy loss inside an active calorimeter without any other activity in the detector. $NA64_e$ at CERN (100) is currently the only experiment exploiting this technique.

For an electron beam experiment, the missing energy technique is challenged by charged current neutrino production beyond 10^{14} eot, where the incoming electron converts into a neutrino and soft recoiling nucleus. Missing momentum relies instead on a change in the transverse momentum of the electron, which is tagged before and after the production process. As such, charged current backgrounds are mitigated (because the scattered electron is tagged), but neutral current neutrino backgrounds are still a challenge beyond 10^{17} eot, depending on beam energy. Another attractive feature of the missing momentum technique is that it is sensitive to the mass of the underlying particles that are produced.

The main challenge of these two approaches is the high required detection efficiency for multi-GeV neutrons and kaons in order to veto events where a hard photon (from the incoming electron) converts into a few-body neutral hadronic final state. This requires detectors with excellent hermeticity in the forward direction and a high-fidelity electromagnetic and hadronic calorimeter. However, these techniques have an intrinsic advantage in sensitivity for the same luminosity compared with techniques that require rescattering or decay of the DM candidate/FIP, as they require neither rescattering nor decay and, therefore, have a sensitivity that scales only as the SM mediator coupling squared, g^2 or ε^2.

4.4. Missing Mass Technique

The missing mass ($\not{M}$) technique is used mostly to detect invisible particles in reactions with well-known initial states, such as (*a*) at e^+e^- collider experiments [Belle II and, in the future, BES III (79)] using the process $e^+e^- \to A'\gamma$, where a single photon is detected and nothing else; (*b*) at kaon factories (NA62) via the decay $K \to \pi X$, where X is either long-lived or decaying to light DM states; and (*c*) at positron fixed-target experiments (PADMEs) via the process $e^+e^- \to A'\gamma$, where the positron annihilates with the electrons in the target and a single photon is detected in the final state and nothing else.

A characteristic feature is the presence of a narrow resonance emerging over a smooth background in the distribution of the missing mass. This technique requires detectors with very good hermeticity to allow full control of the kinematics of the initial and final states. The main limitation of this technique is the knowledge of the background arising from processes in which particles in the final state escape the apparatus without being detected.

5. EXPERIMENTAL SENSITIVITY

Table 3 summarizes the characteristic parameters and signatures in each portal model. In the following sections, for each portal, experimental bounds from past and current searches are compared

Table 3 Main parameters to which each portal is sensitive and relative signatures

Portal	Parameter space	Signature
Dark photon (A')	$y = \alpha_D \varepsilon^2 \alpha (m_\chi / m_{A'})^4$ versus m_χ	DM scattering, $A' \rightarrow$ invisible
	Q_χ / e	$A' \rightarrow$ millicharged fermions
	ε versus $m_{A'}$	$A' \rightarrow$ visible modes
Dark scalar (S)	$\sin\theta$ versus m_S	$S \rightarrow$ visible/invisible modes
Dark pseudoscalar (a)	Photons: $g_{a\gamma\gamma}$ versus m_a	$a \rightarrow$ visible/invisible modes
	Fermions: $g_Y = 2v/f_a$ versus m_a	$a \rightarrow$ visible/invisible modes
	Gluons: $g_G = 1/f_G$ versus m_a	$a \rightarrow$ visible
Heavy neutral lepton (N)	U_e^2, U_μ^2, U_τ^2 versus m_N	$N \rightarrow$ visible/invisible modes

against projections of existing or proposed experiments and bounds from several astrophysical and cosmological sources, computed within the same model (see Section 2.4). It is important to note that astrophysical and cosmological probes tend to be more dependent on the details of the portal model than accelerator-based results, which instead represent a solid ground for benchmarking theoretical hypotheses. The sensitivity projections should be treated with caution because the underlying analyses are rather inhomogeneous in their level of detail and sometimes also in the underlying assumptions.

5.1. Vector Portal: Search for Dark Photons and Light Dark Matter

Motivated by models of light DM, much theoretical and experimental effort over the past decade has focused on the vector portal, which at low energies involves kinetic mixing between the photon and the dark vector, $\varepsilon/2F^{\mu\nu}F'_{\mu\nu}$. This portal has received such attention in part because it is the least constrained scenario that allows for bilinear mixing. It also provides the most scope for model building, including what has become the benchmark model for sub-GeV DM (see, e.g., 3, 4, 6).

As explained in Section 2.2.2, the vector portal allows a minimally coupled viable WIMP-like DM model to be built with a light vector mediator (dark photon, A') and a DM candidate χ. In general, the usual analysis of accelerator-based searches starts from the assumption that the mediator is light enough to be produced on-shell, though off-shell production reactions are also important. The production process of A' depends on the available beam. It can be bremsstrahlung for an electron beam; annihilation with the electrons of a target for a positron beam; or meson decays, bremsstrahlung, and/or deep inelastic scattering for a proton beam line. Experimental signatures depend on the ratio between the vector mediator and DM particle masses, $m_{A'}/m_\chi$. They can be (*a*) for $m_{A'}/m_\chi \geq 2$, an invisible decay of A', $A' \rightarrow \chi\overline{\chi}$, which can be detected via missing energy, missing momentum, and missing mass techniques or via DM scattering off the detector material; or (*b*) for $m_{A'}/m_\chi < 2$, a visible decay of A' into SM final states and direct production of $\chi\overline{\chi}$ through an off-shell A', which again can be detected with missing mass and missing energy techniques.

5.1.1. Light dark matter production. With the experimental effort to fully explore light DM now becoming a reality, it is timely to analyze the full thermal relic parameter space to determine what capabilities are needed to fully test and either discover or exclude simple models of light thermal DM. **Figure 1** shows the lively activity of past, current, and proposed experiments to search for light DM with mass in the MeV–GeV range at accelerator-based experiments in all major laboratories worldwide. Results are compared against the current bounds for DM from

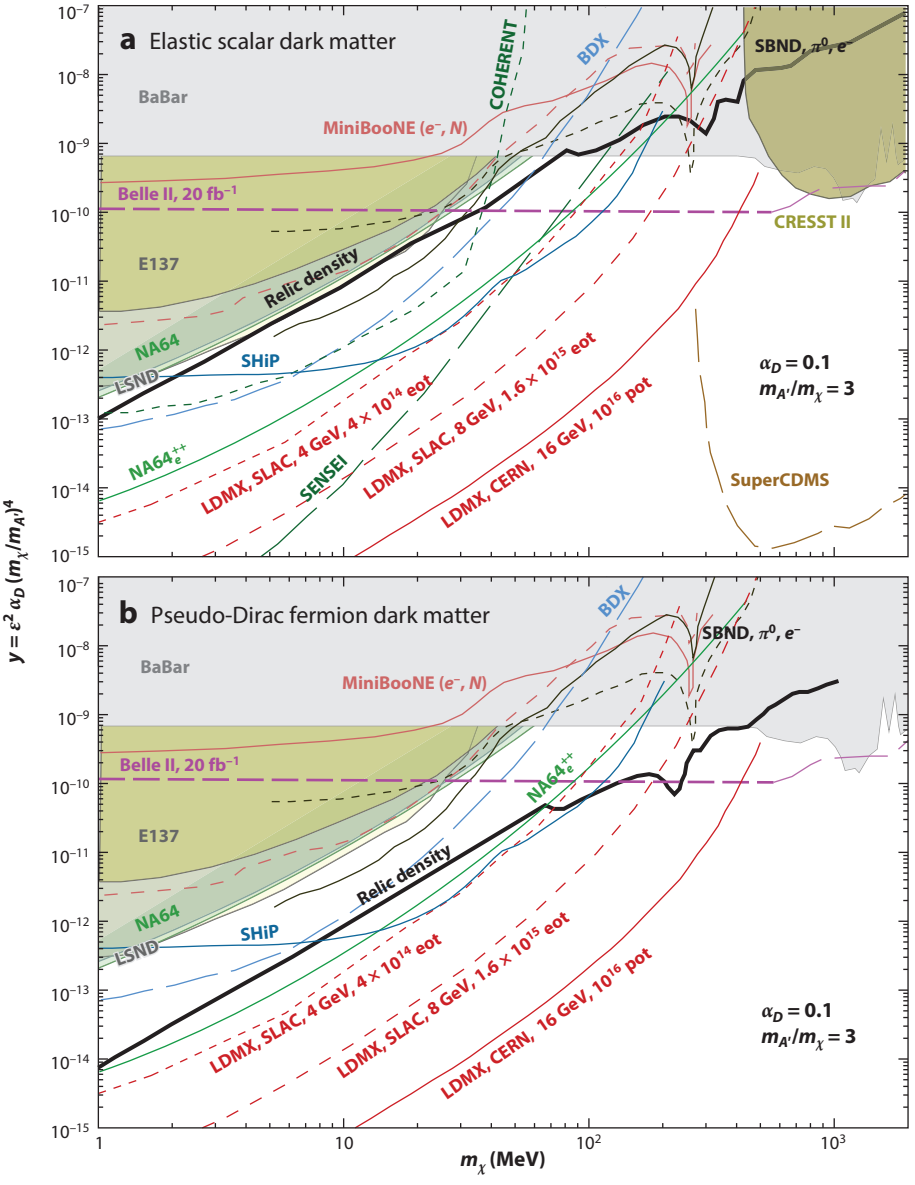

Figure 1

Existing limits (*filled areas*) and future sensitivities of existing or proposed experiments (*colored curves*) to light dark matter (DM) production through a dark photon in the plane defined by the yield variable y as a function of DM mass m_χ for a specific choice of $\alpha_D = 0.1$ and $m_{A'}/m_\chi = 3$. The DM candidate is assumed to be (*a*) an elastic scalar or (*b*) a pseudo-Dirac fermion. Limits shown as filled areas are from BaBar (101), NA64$_e$ (102), reinterpretation of the data from E137 (103) and LSND (62), results from MiniBooNE (104), and CRESST II (inferred sensitivity from the direct detection DM experiment) (61). The projected sensitivities, shown as solid or dashed lines, are from SHiP (15), BDX (22), SBND (84), COHERENT (108), LDMX at SLAC (16, 106), LDMX at CERN (107), Belle II (105), SENSEI (4), and SuperCDMS (109). Figure adapted with permission from Reference 112; copyright 2021 Springer Nature Switzerland AG.

cosmology under the hypothesis that the light DM candidate is a scalar (**Figure 1*a***) or pseudo-Dirac fermion (**Figure 1*b***) particle.

As explained in Section 2.4, for a specific choice of DM particle χ (e.g., scalar, Majorana, pseudo-Dirac), accelerator-based experiments can be directly compared against a reinterpretation of results from DM direct detection experiments. However, the quantitative results of this comparison depend strongly on the spin and other details of the DM particle. As discussed above, the origin of this dependence is connected to the underlying physical reason why accelerator and direct detection techniques are fundamentally complementary: Direct detection probes DM deep in the nonrelativistic limit, whereas accelerator experiments probe DM interactions in the relativistic limit. As a result, different choices of DM spin can lead to direct detection rates suppressed by multiple powers of DM halo velocity $v \sim 10^{-3}$ among different models, whereas accelerator rates are only mildly affected by changing the spin. Thus, to give a representative view of the complementary nature of these techniques, **Figure 1** shows two viable scenarios where the DM spin is different—namely, a scalar and a pseudo-Dirac fermion.

The current bounds shown in **Figure 1** are expressed in the parameter space (y, m_χ) and come from BaBar (101), NA64$_e$ (102), reinterpretation of the data from old beam dump experiments such as E137 (103) and LSND (62), MiniBooNE (104), and—only in the case of scalar DM—interpretation of data from the direct detection experiment CRESST II (61). The projected sensitivities come from SHiP (15), BDX (22), SBND (84), Belle II (105), LDMX at SLAC (16, 106), LDMX at CERN (107), and—again only in the case of scalar DM—some direct detection experiments, such as COHERENT (108), SENSEI (with a proposed 100-g detector) (4), and SuperCDMS (109), the last two of which are expected to be operated at SNOLAB. The existing bounds and projected sensitivities for beam dump experiments do not include the contribution of dark photons that originated from the electromagnetic component in hadronic showers (110) (for proton beams) and from the positron annihilation processes (111) in electromagnetic showers.

The sensitivity plots in **Figure 1** have been obtained for $m_{A'}/m_\chi = 3$ and for the coupling with DM $\alpha_D = 0.1$, which are quite commonly used in literature (though $\alpha_D = 0.5$ is the other common choice). The dependence of the bounds with these two parameters has been extensively studied in Reference 113. While the dependence of the y variable with α_D is implicit in the definition of y, the dependence with $m_{A'}/m_\chi$ is more involved. However, beyond the resonant process occurring at $m_{A'} = 2m_\chi$, the dependence of y is a decreasing function with the mass ratio, and therefore $m_{A'} = 3m_\chi$ generally yields a conservative estimate of experimental sensitivity within the region where the effective field theory is approximately valid at freeze-out. For this conservative choice of α_D and $m_{A'}/m_\chi$ parameters, the region of parameter space corresponding to thermal freeze-out is close to saturated by existing data or will be in the near future if the DM is an elastic scalar particle (**Figure 1*a***). In the case of a pseudo-Dirac fermion DM (**Figure 1*b***), the thermal relic target is still far from the actual experimental bounds but can be reached in the not-too-distant future.

5.1.2. Dark photon decays to visible final states. If the DM is heavier than $m_{A'}/2$ or contained in a different sector, then the A', once produced, decays back to SM particles via the ε-proportional interactions between dark photon and SM particles, as shown in **Figure 2**. Existing limits on the massive dark photon for $m_{A'} > 1$ MeV come from peak searches at collider/fixed-target experiments [A1 (114), LHCb (115), CMS (116), BaBar (117), KLOE (118–121), and NA48/2 (122)] and old beam dump experiments [E774 (65), E141 (64), E137 (63, 103, 123), NuCal (66, 67), and CHARM (124)]. Bounds from supernovae (125) and $(g-2)_e$ (44) are included as well. **Figure 2** also shows projections for existing and proposed experiments on the massive dark photon for $m_{A'} > 1$ MeV: Belle II (105) at SuperKEKb, LHCb upgrade (126, 127) at the LHC, NA62

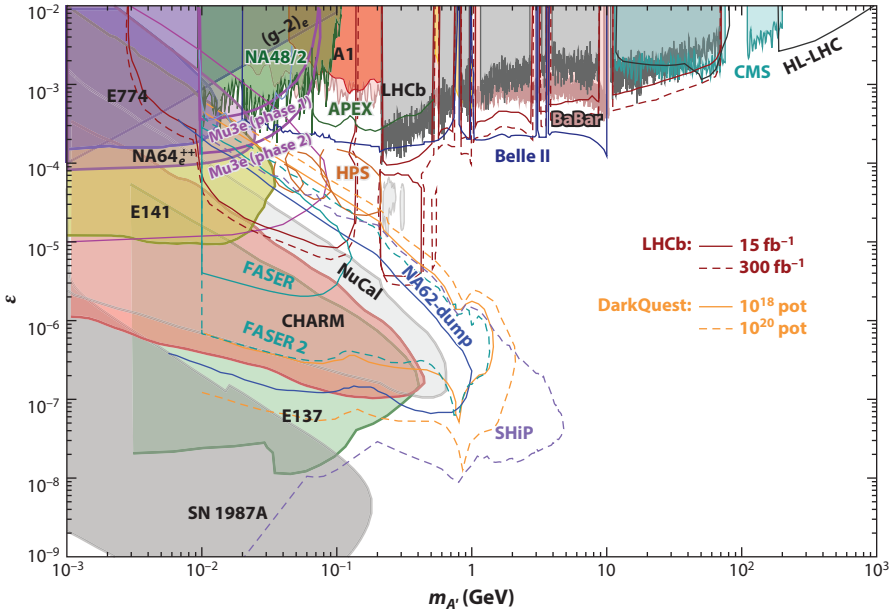

Figure 2

Dark photon decay into visible final states: ε versus $m_{A'}$. Filled areas indicate existing limits from searches at collider/fixed-target experiments [A1 (114), LHCb (115), CMS (116), BaBar (117), and NA48/2 (122)] and old beam dump experiments [E774 (65), E141 (64), E137 (63, 103, 123)), NuCal (66, 67), and CHARM (124)]. Bounds from supernovae (125) and $(g-2)_e$ (44) are also included. Colored curves indicate projections for existing and proposed experiments: Belle II (105), LHCb upgrade (126, 127), NA62 in dump mode (14) and $NA64_e^{++}$ (81), FASER and FASER 2 (91), DarkQuest (85), HPS (128), Mu3e (130), and HL-LHC (131). Figure adapted with permission from Reference 112; copyright 2021 Springer Nature Switzerland AG.

in dump mode (14) and $NA64_e^{++}$ (81) at the SPS, FASER and FASER 2 (91) at the LHC, DarkQuest (85) at Fermilab, HPS (128) at Jefferson Lab, DarkMESA (129) at Mainz, and the Mu3e experiment at PSI (130). For masses above ~100 GeV, projections are obtained for ATLAS/CMS during the high-luminosity phase of the LHC (131).

From **Figure 2** it is apparent that collider-based and beam dump experiments cover a fully complementary region in the parameter space: Collider experiments are mostly sensitive to relatively large couplings and masses, and beam dump experiments are sensitive to lower couplings and masses below the order of a few GeV. The motivated range for ε of 10^{-5} to 10^{-3} and masses less than 1 GeV will be covered in the short future mostly by LHCb, HPS, and Mu3e. Proton beam dump experiments (NA62 in dump mode, DarkQuest, and possibly SHiP) will push the exploration below $\varepsilon \sim 10^{-5}$.

5.1.3. Millicharged particle production. Millicharged particles arise, as discussed in Section 2.2.2, in the case of a massless dark photon because the rotation of the mixing term leaves the photon coupled to the dark sector particles χ with strength $\varepsilon\varepsilon'$. Searches are accordingly parameterized in terms of the mass m_χ and the electromagnetic coupling (modulated by ε) of the supposedly millicharged dark sector particle.

The physics of stellar evolution for horizontal branches, red giants, and white dwarves (132), together with supernovae (133), provides bounds in the region of small masses ($m_\chi < 1$ MeV). In

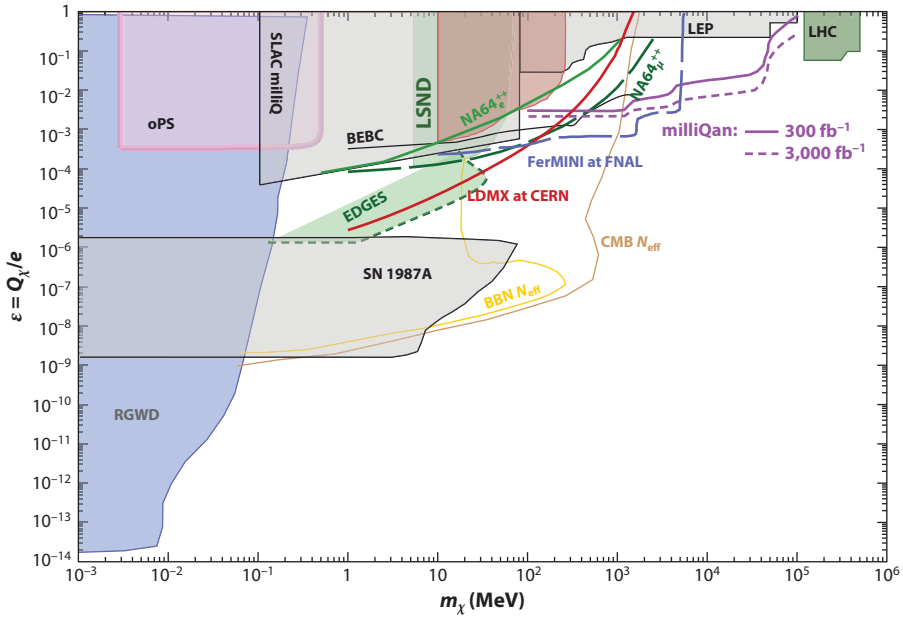

Figure 3

Dark photon millicharged particles. Existing limits (*filled areas*) and future sensitivities for existing or proposed experiments (*curves*) are shown. Existing limits are from stellar evolution [red giants and white dwarves (RGWD) (132) and SN 1987A (133)], N_{eff} during Big Bang nucleosynthesis (BBN) and cosmic microwave background (CMB) (132), invisible decays of ortho-positronium (oPS) (135), the SLAC milliQ experiment (136), reinterpretation of data from LSND and MiniBooNE (137) and from the old BEBC experiment at CERN (138), interpretation of the anomalous 21-cm hydrogen absorption signal by EDGES (141), and searches at LEP (139) and the LHC (140). Future sensitivities are from NA64$_e^{++}$ (81), NA64$_\mu^{++}$ (88), FerMINI (144), milliQan (92), and LDMX (16). Figure adapted with permission from Reference 112; copyright 2021 Springer Nature Switzerland AG.

this region, constraints on N_{eff} during nucleosynthesis and in the CMB [N_{eff} BBN and CMB (132)] limit the possibility of having millicharged particles.

Further limits can be derived from precision measurements in QED, notably from the Lamb shift in the transition $2S_{1/2}$-$2P_{3/2}$ in the hydrogen atom (134) and the nonobservation of the invisible decay of ortho-positronium (oPS) (135). Limits in the intermediate mass range of 1–100 MeV come from a SLAC dedicated experiment (SLAC milliQ) (136), from the reinterpretation of data from the neutrino experiments LSND and miniBooNE (137), and from the old BEBC experiment at CERN (138). Searches at LEP (139) and the LHC (140) cover larger values of the mass (100 MeV $< m_\chi <$ 1 TeV). All these limits are shown as filled areas in **Figure 3**. Millicharged particles as DM have been proposed (see, e.g., 141, 142) to explain the anomalous 21-cm hydrogen absorption signal reported by the EDGES experiment (143).

The projected limits of future experiments are depicted in **Figure 3** as colored curves. Of these, the most significative for masses around 1 GeV come from the proposed milliQan experiment (92), proposed to be installed on the surface above one of the LHC interaction points. The milliQan detector could improve the collider limits by two orders of magnitude. The mass range of 10 to 100 MeV can be optimally covered by the FerMINI experiment (144) proposed in the DUNE Near Detector Hall at Fermilab. Finally, the search for millicharged particles below 10-MeV mass

may be improved by almost two orders of magnitude by the LDMX experiment (16) that has been proposed both at CERN (107) and at SLAC (106).

5.2. Scalar Portal: Search for Light Scalar Particles Mixing with the Higgs Boson

In a minimal scalar portal model, the new singlet scalar has a quadratic coupling λ_{HS} and a mixing term to the Higgs $\sin\theta$, as detailed in Section 2.2.3. The light scalar production always occurs via the Higgs boson, both on- and off-shell. If the Higgs is on-shell, the production is dominated by the quartic coupling, λ_{HS}, via the direct decay $H \to SS$. This process is instead subdominant when the Higgs is off-shell. In this case, the production occurs via Higgs penguin diagrams (e.g., $K \to \pi S$ and $B \to KS$ decays) with a probability proportional to $\sin^2\theta$. The mixing term also drives the light scalar decays.

The production processes also define the maximum light scalar mass that can be explored at different experimental facilities: up to $m_K - m_\pi$ for kaon factories and proton beam dump experiments (if the center-of-mass energy $\sqrt{s}$ is sufficient for production of a pair of strange particles); up to $m_B - m_K$ for b factories, LHCb, and proton beam dump experiments (if $\sqrt{s}$ is more than twice the b quark mass); and up to $m_b/2$ for LHC-based experiments.

The current experimental bounds and future projections in the plane $\sin^2\theta$ versus m_S are shown in **Figure 4**. First investigation of light dark scalars with masses below the kaon threshold has been conducted by reinterpreting (145) the results from the CHARM experiment (146). Masses below the kaon mass can be optimally explored at kaon factories [E949 (147), NA62 (148)] and possibly in the future by the KLEVER (6) experiment as by-products of the $K \to \pi\nu\bar{\nu}$ analyses using the missing mass technique and assuming the two-body decay $K \to \pi S$, where S is not detected. NA62 and KLEVER should be able to close the gap between the current E949 bound and constraints arising from SN 1987A (see discussion below). MicroBooNE (149) recently set a bound between 100 and 200 MeV that excludes a light feebly interacting scalar as responsible for the KOTO anomaly[1] (150).

Light scalars with masses between the kaon and the B meson mass have been searched for at LHCb (152, 153) and Belle (154) via the decays $B^{+,0} \to K^{+,*0}S$, $S \to \mu^+\mu^-$. Both LHCb and Belle II are expected to improve over these limits in the coming years. In the same mass range, in the close future, NA62 in dump mode (14) and DarkQuest (17)—and, on a longer timescale, Belle II (155) with 50 ab^{-1} and possibly SHiP (15)—will be able to push the exploration of the parameter space toward smaller couplings. Experiments at the LHC, such as FASER 2 (11), CODEX-b (9), MATHUSLA (13), and ANUBIS (98), will possibly extend the sensitivity for dark scalars up to half of the Higgs mass. For LHC-based detectors, projections are obtained assuming the quartic coupling fixed to $\lambda_{HS} \sim 6 \times 10^{-4}$, which corresponds to the precision ($\sim$1%) obtainable on the invisible Higgs branching fraction by a future e^+e^- circular collider (8).

The jump in sensitivity at $\sim$200 MeV and then at $\sim$3.8 GeV shown in **Figure 4** is due to the opening of the $\mu^+\mu^-$ and $\tau^+\tau^-$ thresholds, respectively, as this portal inherits from the SM its Yukawa structure. The complicated structure at $\sim$1 GeV is defined by the inclusion of resonant $\pi\pi$ final states whose rate is still known only with large uncertainties (145).

Finally, in the limit of small mixing angle, one can bound the quartic coupling λ_{HS} via the Higgs invisible branching fraction, since λ_{HS} is naturally expected to satisfy the relation $\lambda_{HS} \leq m_S^2/v^2$.

[1]At the KAON 2019 conference (**https://indico.cern.ch/event/769729/**), the KOTO Collaboration announced a preliminary observation of four events with an expectation background of 0.05 ± 0.02 in the search for $K_L \to \pi^0\nu\bar{\nu}$ decays.

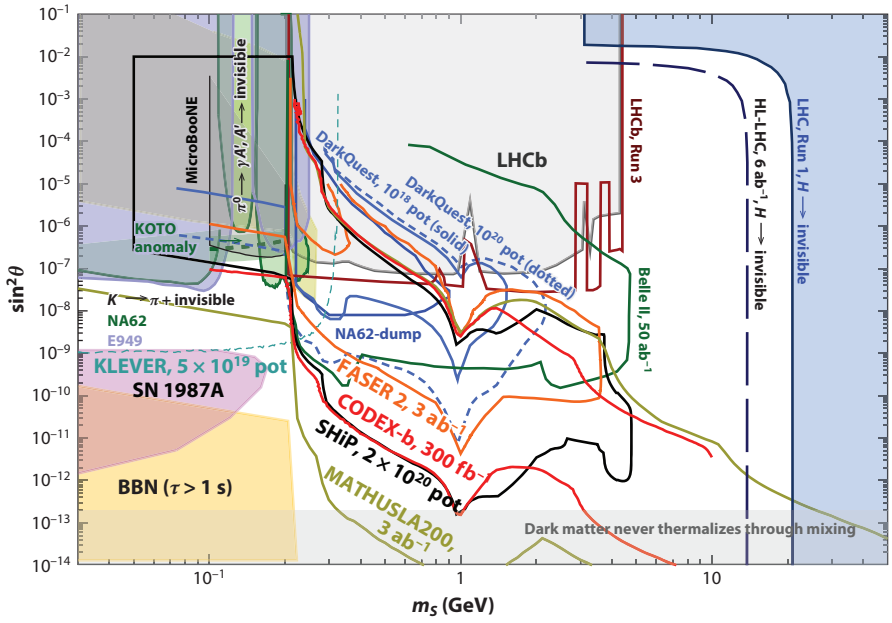

Figure 4

Dark scalar decay into visible final states. Existing limits (*shaded areas*) come from reinterpretation (145) of results from NA62 (148); E949 (147, 151); MicroBooNE (149), which excludes a light dark scalar as an interpretation (150) of the KOTO anomaly; and LHCb (152, 153). Colored lines indicate projections from existing or proposed experiments: NA62 in dump mode (14) and DarkQuest (17), Belle II (155), SHiP (15), FASER 2 (11), CODEX-b (9), MATHUSLA (13), and KLEVER (6). The vertical lines correspond to the bounds obtainable on λ_{HS} based on knowledge of the invisible Higgs width after Run 1 at the LHC and projections in the HL-LHC era (see 8 and references therein). Big Bang nucleosynthesis (BBN) and SN 1987A data are from References 156 and 157, respectively.

The vertical lines in **Figure 4** correspond to the bounds obtainable on λ_{HS} based on knowledge of the invisible Higgs branching fraction from ATLAS and CMS after LHC Run 1 and projections in the HL-LHC era (see 8 and references therein).

As discussed in Section 2.4, light dark scalars also can be constrained by astrophysics sources. A light (<100 MeV) dark scalar with a thermal number density can decay during BBN and spoil the successful predictions of light element yields accumulated in the early Universe (156). Likewise, a light dark scalar produced on-shell during a supernova explosion can significantly contribute to its energy loss, thereby shortening the duration of the observable neutrino pulse emitted during core collapse (see, e.g., 157).

Light dark scalars also can be mediators between DM χ and SM particles. However, it has been demonstrated (157, 158) that for mediator masses $m_S \geq 2m_\chi$, DM annihilating directly into SM particles is ruled out by low-energy experiments for nearly all DM candidates under the most conservative assumptions regarding the DM mediator couplings and mass ratios. If the mediator is lighter than m_χ and the relic abundance is set by secluded annihilation $\chi\overline{\chi} \to SS$, then the $\sin\theta$ mixing parameter is only bounded from below by the DM thermalization requirement ($\sin^2\theta > 10^{-13}$) (157), and the parameter space is still open for exploration.

Nonminimal models that could explain the Higgs hierarchy problem (neutral naturalness, twin Higgs, relaxion) or originate a strong EW phase transition include the scalar portal as a

connection between New Physics and SM particles. These models have similar phenomenology to the minimal one and can provide important target areas for future searches.

5.3. Pseudoscalar Portal: Search for Heavy Axions and Axion-like Particles

As explained in Section 2.2.5, ALPs can mediate interactions between DM and the SM sector via three different couplings: photon, gluon, and fermion coupling. In this review, only experimental results related to photon coupling are considered. In this case, all the ALP phenomenology (production, decay, oscillation in magnetic field) is fully defined in the $(m_a; |g_{a\gamma}| = f_a^{-1})$ parameter space. A thorough study of the current bounds for ALPs with gluon coupling with mass in the MeV–GeV range can be found in Reference 159.

Searches for axions with photon couplings in the sub-eV mass range have literally exploded in the recent past. The most updated review on laboratory searches for very light axions and ALPs is contained in Reference 6 (see also 160). **Figure 5** shows the sensitivity of current and future experiments to axions and ALPs with photon coupling over about 20 orders of magnitude in mass and about 14 orders of magnitude in coupling.

The contribution from accelerator-based experiments below a mass scale of a few GeV is highlighted in the red box in **Figure 5*a*** and shown in greater detail in **Figure 5*b***. This region of parameter space is particularly interesting because it covers the motivated MeV–GeV region that is still compatible with the QCD axion band. Searches for ALPs with photon coupling have been performed at e^+e^- collider-based experiments using monophoton searches ($e^+e^- \to \gamma^* \to a\gamma$) at LEP (for data, see 169–172; for interpretation, see 173) and, recently, using triphoton searches in the process $e^+e^- \to \gamma a, a \to \gamma\gamma$ at Belle II (174) with $\sim$0.5 fb^{-1} of integrated luminosity.

In electron beam dump experiments [E141 (see 64 for data and 175 for interpretation), E137 (63), and NA64 (176)] and proton beam dump experiments [CHARM (124) and NuCal (177)], the ALPs are supposed to be produced mainly via the Primakoff effect—that is, the conversion of a photon into an ALP in the vicinity of a nucleus (178). In the close future, NA62 in dump mode, NA64$_e^{++}$ (81), and FASER should be able to improve over the current results for masses below 1 GeV. The Primakoff effect is also the dominant production mechanism for ALPs with photon coupling in photon beam dump experiments such as PrimEx (179) and GlueX (see **https://www.jlab.org/exp_prog/proposals/17/PR12-17-007.pdf**) at Jefferson Lab. A study of their physics reach has been performed in Reference 180.

The ATLAS and CMS Collaborations are currently searching for ALPs with photon couplings in a relatively higher mass region, $5 < m_a <$ 100s of GeV, using exclusive diphoton final states [as, for example, in the process pp, $PbPb \to \gamma\gamma \to a(\gamma\gamma)$] (181–183), inclusive $\gamma\gamma$ resonances [as in $pp \to Z \to a(\gamma\gamma)\gamma$] (184), and exotic Z or Higgs decays [as in $pp \to H \to a(\gamma\gamma) + Z, \gamma$ or $pp \to H \to a(\gamma\gamma) + a(\gamma\gamma)$] (185–187).

Constraints on the photon-ALP coupling also arise from the study of the neutrino signal from SN 1987A, where axions or ALPs with masses up to about 100 MeV, possibly copiously produced in the hot core of a supernova, could constitute a new energy loss mechanism (188).

5.4. Fermion Portal: Search for Heavy Neutral Leptons

HNLs can be produced in any process involving neutrinos in the final states, such as pion, kaon, D and B meson, and Z decays, with a probability proportional to the mixing parameters $|U_{e,\mu,\tau}|^2$. Once produced, the HNLs can decay via charged current and neutral current interactions into active neutrinos and other visible final states as pions, muons, and electrons.

Heavy neutrinos mixing with the first and second lepton generations, ν_e and ν_μ, can be searched for in the missing mass distribution of pion and kaon leptonic decays [e.g., $K, \pi \to \mu(e)^+ \nu_\mu\ (\nu_e)$]. These searches are very robust because they assume only that an HNL mixes with ν_e and ν_μ. Another strategy to search for HNLs is via searches of their decay products. This is the typical technique used in proton beam dump experiments where the HNL production process is not known. Results obtained with this technique are in general less robust than those obtained using the missing mass technique because they would be largely weakened if the HNLs had unknown

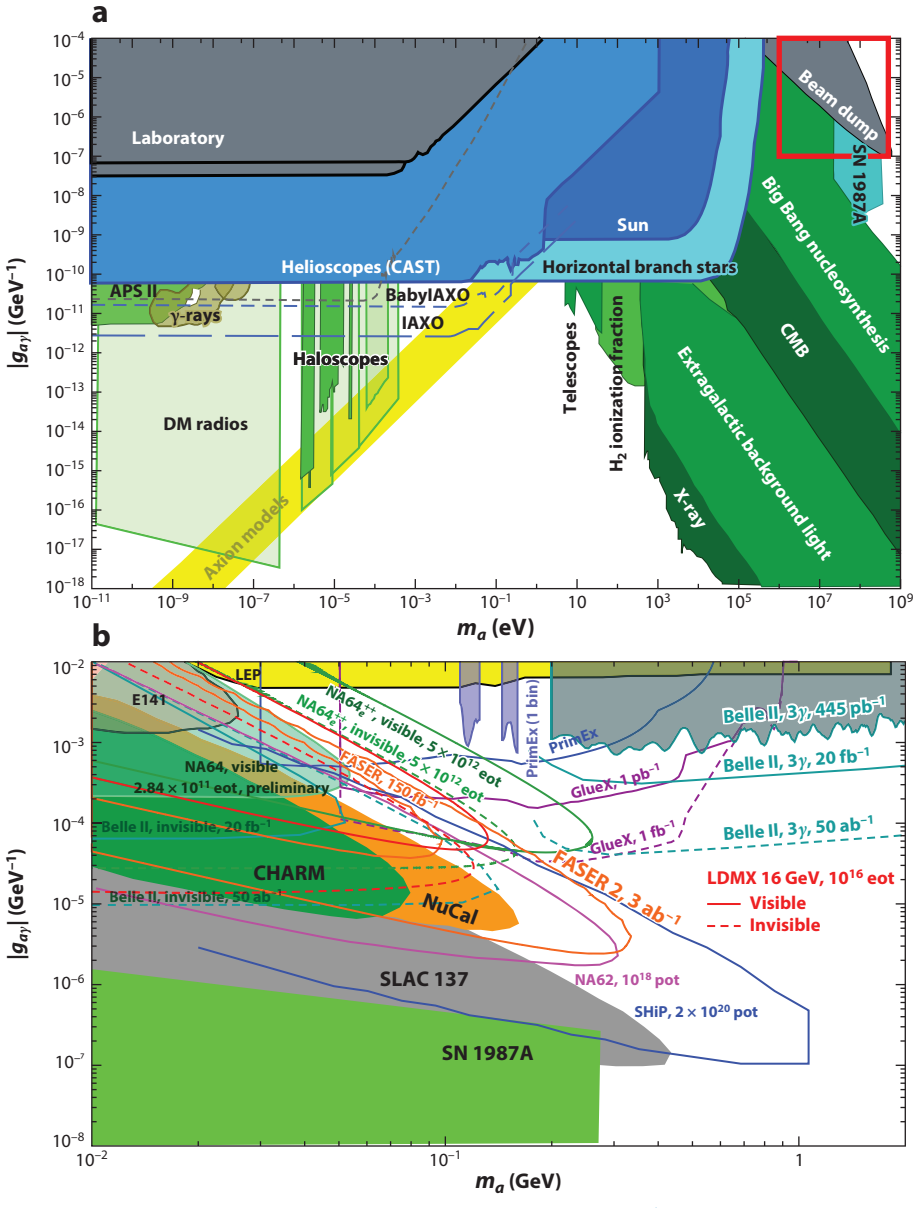

(*Caption appears on following page*)

Figure 5 (*Figure appears on preceding page*)

Axions and axion-like particles (ALPs) with photon coupling. (*a*) Overall view of axion and ALP searches. (*b*) Magnified view of the region of interest for accelerator-based experiments (note the different units for the mass ranges in panels *a* and *b*). The figure follows a color scheme to present results obtained with different methods: black and gray for laboratory results, blue shades for searches for axions from the sun (helioscopes) and bounds related to stellar physics, and green shades for searches for axions as potential dark matter (DM) candidates (haloscopes) or cosmology-dependent arguments (for details, see 6). Hinted regions, like the QCD axion, are in yellow. Laboratory limits (*dark gray areas*) are essentially due to the results of OSQAR (161) (region below 1 meV) and PVLAS (162) (region above 1 meV). The bounds from helioscope and haloscope experiments are driven mostly by CAST (163) and ADMX (164) results. Projections for laboratory experiments, helioscopes, and haloscopes (shown as *gray*, *blue*, and *green dashed curves*, respectively) are dominated by ALPS II (165), IAXO (166) (and its smaller version, BabyIAXO), DM radio (167), and ADMX and MADMAX (168). Shaded areas indicate excluded regions from LEP (for data, see 169–172; for interpretation, see 173), Belle II (174), E141 (for data, see 64; for interpretation, see 175), NA64 (176), CHARM (124), NuCal (177), and PrimEx (180, based on 179). Curves indicate projections from Belle II (105) for 20 fb^{-1} and 50 ab^{-1}, SHiP (15), FASER and FASER 2 (6), NA64$_e^{++}$ (81) in visible and invisible modes, and interpretation of the physics reach (180) of the PrimEx (179) and GlueX experiments at Jefferson Lab. Figure adapted from Reference 6 (CC BY 4.0); revised by I. Irastorza.

decay modes into invisible particles. Another way to constrain the couplings of HNLs in a relatively high mass regime is to use possible Z^0 decays into heavy neutrinos from LEP data. In this case, only large values of the mixing angles can be explored.

The techniques described above assume that HNLs are on-shell particles that can be seen either via visible decays or by using the missing mass technique. These are commonly called direct searches. However, HNLs also can be searched for via precision tests or searches for rare processes in the SM that are indirectly affected through the modification of the active neutrino interactions via the mixing with HNLs (indirect searches). In fact, because of the presence of sterile neutrinos, the mixing matrix of the three active neutrinos is effectively nonunitary. The subsequent modification of the weak currents then leads to modified predictions for EW observables (e.g., the Fermi constant G_F or the Weinberg angle $\sin\theta_W$) compared with the SM. However, in the mass range considered in this work (0.1–100 GeV), direct searches dominate the sensitivity.

In this review we assume, for simplicity, that only one coupling is switched on at the time. Future studies will include combinations of coupling ratios compatible with the active neutrino mixing parameters (see, e.g., 189, 190). **Figure 6** shows the current bounds and sensitivity projections for HNLs coupled to the first (**Figure 6*a***) and third (**Figure 6*b***) lepton flavor generations. Strong constraints on couplings for HNLs with masses below the kaon mass are set by past experiments, in particular PS191 (191), CHARM (146), NuTeV (192), E949 (193), PIENU (194), TRIUMF (195), and NA3 (196). A new analysis of $10^7 \pi^+ \to e^+ \nu_e$ decays by the PIENU collaboration (197) has produced the most stringent limit of $|U_e|^2$ below the pion threshold. The off-axis near detector of the T2K experiment ND280 [with 12.34×10^{20} pot in ν mode and 6.3×10^{12} pot in anti-ν mode (198)] and the NA62 experiment [with 3.5×10^{12} $K^+ \to e^+ \nu_e$ decays in the fiducial volume (199)] have pushed the exploration of the HNL couplings down to approximately the 10^{-9} level for masses up to the kaon mass.

It is important to note that both the BBN and seesaw bounds are meaningful only if more than one HNL-active neutrino coupling is at work, and they should not be considered for the single-flavor dominance case studied in this manuscript. However, they are included in **Figure 6** to show that all the couplings are bounded from below as soon as two HNLs are at work. Above the kaon mass, the current constraints on $|U_e|^2$ weaken significantly; they are dominated by results from the old CHARM experiment up to the charm threshold, by Belle (200) up to the b threshold, and by DELPHI (201), ATLAS (202), and CMS (203) up to the Z threshold.

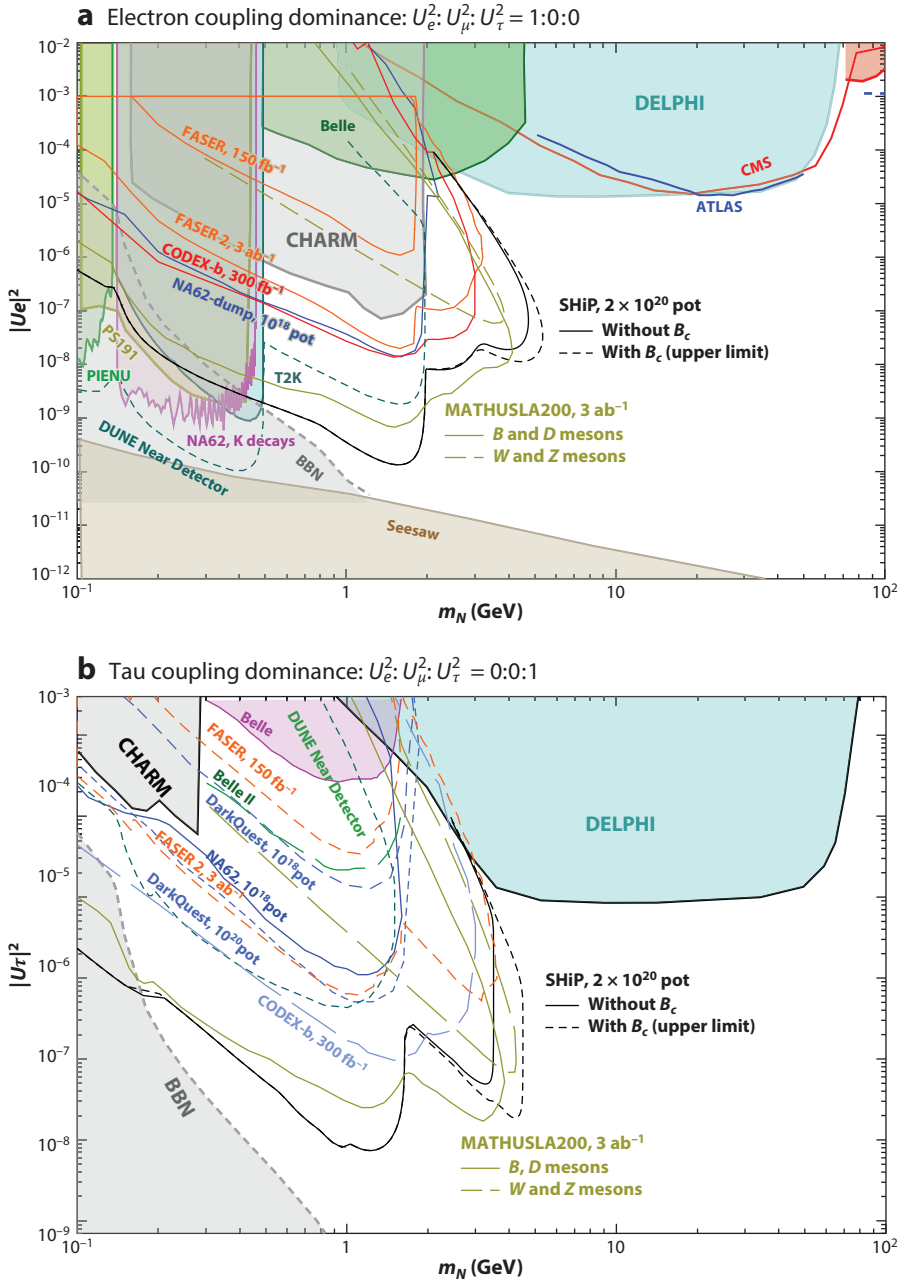

Figure 6

Heavy neutral leptons (HNLs) with coupling to the (*a*) first and (*b*) third lepton generations. Filled areas indicate existing bounds from PS191 (191), CHARM (146), PIENU (197), Belle (200), DELPHI (201), ATLAS (202), and CMS (203). Colored curves indicate projections from NA62 in dump mode (6, 14), DarkQuest (17), Belle II (204), FASER and FASER 2 (91), SHiP (15), DUNE Near Detector (205), CODEX-b (9), and MATHUSLA200 (13). Big Bang nucleosynthesis (BBN) (206) and seesaw bounds are computed under the hypothesis of two HNLs mixing with active neutrinos.

On the timescale of approximately the next 5 years, NA62 in dump mode (189) and DarkQuest (17) (only for $|U_\tau|^2$) can improve the bounds from the CHARM experiment below the charm threshold and be competitive with the projections for FASER and FASER 2 (91), while a significant improvement in the entire mass range below the B meson mass could be achieved on a longer timescale by SHiP (15), Belle II (204), DUNE Near Detector (205), CODEX-b (9), and MATHUSLA200 (13). On a much longer timescale, experiments at future high-energy hadron and lepton colliders will be sensitive to HNLs well beyond the b meson mass via direct and indirect searches (for a summary, see 8).

6. CONCLUSIONS AND OUTLOOK

In recent years, the physics of FIPs and dark sectors has received considerable and growing attention from the broader high-energy physics community. This increased attention has been motivated both by existing data and by the appeal of simple extensions of the SM to address longstanding puzzles in which FIPs play an important role. While a broad mass range is interesting, in this article special focus has been placed on the relatively poorly explored MeV–GeV scale for several reasons, and a systematic investigation of this mass range is now underway. To date, the research programs in this direction have largely occurred in a manner parasitic to other research goals or have been focused on the reinterpretation of old data sets. Relatively few dedicated experiments are currently running, though the number planned and expected to run in the coming years has grown considerably. Nevertheless, the wealth of results produced in the past 5–10 years allows us to draw several noteworthy conclusions:

- Results from the dedicated experiment NA64$_e$ as well as recent proton beam dump searches for light DM in the MeV–GeV range have begun to exclude new parameter space below 100 MeV in certain specific (but well-motivated) models where direct thermal freeze-out can explain the DM abundance (**Figure 1**). The use of a high-energy positron beam with the NA64$_e$ setup would further enhance the sensitivity to light DM searches.
- Dedicated searches for dark photons have excluded the interesting parameter range where a dark photon could be responsible for the $(g-2)_\mu$ anomaly (**Figure 2**).
- HNLs coupled to the first and second SM lepton generations and with masses below the kaon mass are excluded by NA62 and T2K searches down to 10^{-9} (**Figure 6**). These bounds, computed under the simplistic assumption of single-flavor dominance, exclude most of the parameter space below the kaon mass allowed by BBN and seesaw constraints.
- Heavy ALPs with masses between ten and a few hundred MeV are excluded for photon couplings compatible with the QCD axion band (**Figure 5**).
- A light dark scalar acting as the mediator between the SM and DM in s-channel thermal freeze-out DM annihilation has been ruled out—in its minimal form—by low-energy experiments running at b or kaon factories. Significant parameter space for secluded annihilation ($\chi\chi \rightarrow$ pair of mediators $\rightarrow$ SM) is still open above the cosmological bound of $\sin^2\theta > 10^{-13}$ (**Figure 4**).

In the next 10 years, a multitude of new initiatives (or upgrades of ongoing experiments) will produce a large set of results applicable to FIP and dark sector physics. In parallel, ongoing theoretical work is providing guidance with respect to regions of parameter space in minimal models that are deserving of special attention. Advanced calculations of FIP production and decay rates and the inclusion of more complete bounds from astrophysical and cosmology data will all be important to properly interpret the wave of new data expected in the coming years. Though the future

is not always straightforward to predict, we expect several interesting milestones to be reached by upcoming experiments in the next 10 years:

- Most of the parameter space below $\mathcal{O}(300)$ MeV where direct thermal freeze-out can explain the DM abundance (for both scalar and fermion DM models interacting through a light DP) will be explored by dedicated searches, such as LDMX at SLAC, NA64 at CERN, and beam dump experiments at FNAL and Jefferson Lab. Likewise, Belle II is expected to probe the region above $\mathcal{O}(300)$ MeV. Additionally, direct detection sensitivity will be extended by a series of new experiments including SENSEI, DAMIC, and SuperCDMS. Taken together, these experiments will broadly extend sensitivity to WIMP-like DM deep into the sub-GeV range, analogous to the way in which the LHC and large-scale direct detection experiments will probe the mass range of hundreds of GeV to TeV.
- Important regions of the parameter space for the QCD axion and ALPs will be explored in the coming years (**Figure 5**). In particular, helioscopes will improve sensitivity to axions and ALPs to probe parts of parameter space consistent with recent hints regarding anomalous energy loss channels in stars and/or anomalous γ-ray transparency of the Universe. Haloscopes will complement this quest by increasing sensitivity down to the range of coupling and mass at which the QCD axion can be a DM candidate. In addition, much of the ALP parameter space where simple misalignment predicts the correct DM density will be explored (e.g., by ADMX and DM radio). Finally, accelerator-based experiments will continue to explore the well-motivated QCD scale (MeV–GeV) and beyond at larger ALP couplings.
- Searches for HNLs will be performed by NA62 in dump mode, DarkQuest, Belle II, and LHC-based experiments in the still mostly uncharted region above the kaon mass in a range of couplings compatible with successful leptogenesis.

The field of FIPs and dark sectors is still fresh, and many possible avenues can and should be pursued in the future. Theoretical studies should continue to map out how the known portal operators are embedded in complete models addressing the varied puzzles of the SM, and this knowledge will be important in identifying additional promising sensitivity milestones around which to focus experimental efforts. At the same time, such studies will naturally motivate the inclusion of less minimal models with more complicated signatures in future searches. Within the context of even the minimal models described in this review, much work remains to be carried out on the comparison of the results from different experiments. For example, understanding the interplay between active neutrino mixing parameters derived from ongoing and future neutrino experiments and the favored ranges of HNL parameters would be important, as would more comprehensive comparisons of sub-GeV direct detection searches and accelerator-based searches. Likewise, the wealth of data coming from accelerator-based experiments should be compared in greater detail with existing and future astrophysics- and cosmology-driven sources of insight.

Given the apparent absence of new TeV-scale physics at the LHC in the form predicted by low-energy supersymmetry, the field of high-energy physics is in the midst of stepping back to reconsider other promising approaches to open questions in particle physics. Going forward, addressing these fundamental and interconnected questions requires a diversified and cross-frontier research program that incorporates accelerator physics, underground detectors, cosmology and astrophysics instruments, and precision experiments, all supported by a strong and focused theoretical involvement. In this vein, the field of FIPs and dark sector physics is casting a light on the sub-GeV frontier and offers many opportunities for exciting and profound discoveries in the future.

DISCLOSURE STATEMENT

The authors are not aware of any affiliations, memberships, funding, or financial holdings that might be perceived as affecting the objectivity of this review.

ACKNOWLEDGMENTS

We acknowledge the use of the DARKCAST package (**https://gitlab.com/philten/darkcast**) for some of the numerical results shown in this review. G.L. warmly thanks the BSM Working Group of the Physics Beyond Colliders initiative and the speakers and organizing committee of the FIPs 2020 and PBC Meets Theory workshops for the lively discussions about most of the topics covered in this review. M.P. is supported in part by the US Department of Energy (grant desc0011842). P.S. is supported by the US Department of Energy under contract DE-AC02-76SF00515.

LITERATURE CITED

1. Feng JL, et al. arXiv:1401.6085 [hep-ex] (2014)
2. Hewett JL, et al. arXiv:1401.6077 [hep-ex] (2014)
3. Alexander J, et al. arXiv:1608.08632 [hep-ph] (2016)
4. Battaglieri M, et al. arXiv:1707.04591 [hep-ph] (2017)
5. Alimena J, et al. *J. Phys. G* 47:090501 (2020)
6. Beacham J, et al. *J. Phys. G* 47:010501 (2020)
7. Argüelles CA, et al. *Rep. Prog. Phys.* 83:124201 (2020)
8. Ellis RK, et al. arXiv:1910.11775 [hep-ex] (2020)
9. Aielli G, et al. *Eur. Phys. J. C* 80:1177 (2020)
10. Ariga A, et al. arXiv:1812.09139 [physics.ins-det] (2018)
11. Ariga A, et al. *Phys. Rev. D* 99:095011 (2019)
12. Alpigiani C, et al. arXiv:1811.00927 [physics.ins-det] (2018)
13. Alpigiani C, et al. arXiv:2009.01693 [physics.ins-det] (2020)
14. NA62 Collab. *Addendum I to P326: continuation of the physics programme of the NA62 experiment*. Rep. CERN-SPSC-2019-039/SPSC-P-326-ADD-1, CERN, Geneva (2019)
15. Anelli M, et al. arXiv:1504.04956 [physics.ins-det] (2015)
16. Åkesson T, et al. arXiv:1808.05219 [hep-ex] (2018)
17. Batell B, Evans JA, Gori S, Rai M. arXiv:2008.08108 [hep-ph] (2020)
18. Berryman JM, et al. *J. High Energy Phys.* 2002:174 (2020)
19. Kahn Y, Krnjaic G, Tran N, Whitbeck A. *J. High Energy Phys.* 1809:153 (2018)
20. Christmann B, et al. *Nucl. Instrum. Meth. A* 958:162398 (2020)
21. Raggi M, Kozhuharov V, Valente P. *EPJ Web Conf.* 96:01025 (2015)
22. Battaglieri M, et al. arXiv:1607.01390 [hep-ex] (2016)
23. Kolb R, et al. *Basic research needs for dark matter small projects: new initiatives*. Rep., US Dep. Energy, Washington, DC. **https://science.osti.gov/-/media/hep/pdf/Reports/Dark_Matter_New_Initiatives_rpt.pdf** (2018)
24. Barger V, Giudice GF, Han T. *Phys. Rev. D* 40:2987 (1989)
25. Wells JD. *Phys. Rev. D* 71:015013 (2005)
26. Arkani-Hamed N, Dimopoulos S. *J. High Energy Phys.* 0506:073 (2005)
27. Chacko Z, Goh H-S, Harnik R. *Phys. Rev. Lett.* 96:231802 (2006)
28. Burdman G, Chacko Z, Goh H-S, Harnik R. *J. High Energy Phys.* 0702:009 (2007)
29. Arkani-Hamed N, Dimopoulos S, Dvali G. *Phys. Lett. B* 429:263 (1998)
30. Graham PW, Kaplan DE, Rajendran S. *Phys. Rev. Lett.* 115:221801 (2015)
31. Patt B, Wilczek F. arXiv:hep-ph/0605188 (2006)
32. Silveira V, Zee A. *Phys. Lett. B* 161:136 (1985)

33. Crewther RJ, Di Vecchia P, Veneziano G, Witten E. *Phys. Lett. B* 88:123 (1979). Erratum. *Phys. Lett. B* 91:487 (1980)
34. Peccei RD, Quinn HR. *Phys. Rev. Lett.* 38:1440 (1977)
35. Weinberg S. *Phys. Rev. Lett.* 40:223 (1978)
36. Wilczek F. *Phys. Rev. Lett.* 40:279 (1978)
37. Minkowski P. *Phys. Lett. B* 67:421 (1977)
38. Kuzmin VA, Rubakov VA, Shaposhnikov ME. *Phys. Lett. B* 155:36 (1985)
39. Fukugita M, Yanagida T. *Phys. Lett. B* 174:45 (1986)
40. Akhmedov EK, Rubakov VA, Smirnov AY. *Phys. Rev. Lett.* 81:1359 (1998)
41. Boehm C, Ensslin T, Silk J. *J. Phys. G* 30:279 (2004)
42. Boehm C, Fayet P. *Nucl. Phys. B* 683:219 (2004)
43. Pospelov M, Ritz A, Voloshin MB. *Phys. Lett. B* 662:53 (2008)
44. Pospelov M. *Phys. Rev. D* 80:095002 (2009)
45. Arkani-Hamed N, Finkbeiner DP, Slatyer TR, Weiner N. *Phys. Rev. D* 79:015014 (2009)
46. Pospelov M, Ritz A. *Phys. Lett. B* 671:391 (2009)
47. Nollett KM, Steigman G. *Phys. Rev. D* 89:083508 (2014)
48. Batell B, Pospelov M, Ritz A. *Phys. Rev. D* 80:095024 (2009)
49. Alekhin S, et al. *Rep. Prog. Phys.* 79:124201 (2016)
50. Arkani-Hamed N, Weiner N. *J. High Energy Phys.* 0812:104 (2008)
51. Baumgart M, et al. *J. High Energy Phys.* 0904:014 (2009)
52. Slatyer TR, Padmanabhan N, Finkbeiner DP. *Phys. Rev. D* 80:043526 (2009)
53. Izaguirre E, Krnjaic G, Schuster P, Toro N. *Phys. Rev. D* 88:114015 (2013)
54. Willey RS, Yu HL. *Phys. Rev. D* 26:3086 (1982)
55. Curtin D, Meade P, Yu CT. *J. High Energy Phys.* 1411:127 (2014)
56. Kozaczuk J, Ramsey-Musolf M, Shelton J. *Phys. Rev. D* 101:115035 (2020)
57. Dodelson S, Widrow LM. *Phys. Rev. Lett.* 72:17 (1994)
58. Fayet P. *Phys. Rev. D* 74:054034 (2006)
59. Mohapatra RN, Senjanovic G. *Phys. Rev. D* 23:165 (1981)
60. Strassler MJ, Zurek KM. *Phys. Lett. B* 651:374 (2007)
61. Angloher G, et al. *Eur. Phys. J. C* 76:25 (2016)
62. deNiverville P, et al. *Phys. Rev. D* 84:075020 (2011)
63. Bjorken JD, et al. *Phys. Rev. D* 38:3375 (1988)
64. Riordan EM, et al. *Phys. Rev. Lett.* 59:755 (1987)
65. Bross A, et al. *Phys. Rev. Lett.* 67:2942 (1991)
66. Blümlein J, Brugger J. *Phys. Lett. B* 701:155 (2011)
67. Blümlein J, Brunner J. *Phys. Lett. B* 731:320 (2014)
68. Winter K. Study of a new detector for neutrino electron scattering. In *Proceedings of the Workshop on SPS Fixed Target Physics for the Years 1984–1989*, Vol. 2, ed. I Mannelli, pp. 170–79. Geneva: CERN (1983)
69. Aguilar-Arevalo AA, et al. *Nucl. Instrum. Meth. A* 599:28 (2009)
70. Adinolfi M, et al. *Nucl. Instrum. Meth. A* 488:51 (2002)
71. Adinolfi M, et al. *Nucl. Instrum. Meth. A* 482:364 (2002)
72. Fanti V, et al. *Nucl. Instrum. Meth. A* 574:433 (2007)
73. Abashian A, et al. *Nucl. Instrum. Meth. A* 479:117 (2002)
74. Aubert B, et al. *Nucl. Instrum. Meth. A* 479:1 (2002)
75. Aad G, et al. *J. Instrum.* 3:S08003 (2008)
76. Chatrchyan S, et al. *J. Instrum.* 3:S08004 (2008)
77. Alves AA, et al. *J. Instrum.* 3:S08005 (2008)
78. Abe T, et al. arXiv:1011.0352 [physics.ins-det] (2010)
79. Ablikim M, et al. *Chin. Phys. C* 44:040001 (2020)
80. Cortina Gil E, et al. *J. Instrum.* 12:P05025 (2017)
81. Banerjee D, et al. *Addendum to the NA64 proposal: search for the* $A' \to$ *invisible and* $X \to e^+e^-$ *decays in 2021*. Rep. CERN-SPSC-2018-004, CERN, Geneva. **http://cds.cern.ch/record/2300189?ln=en** (2018)

82. Celentano A, et al. *J. Phys. Conf. Ser.* 556:012064 (2014)
83. Abrahamyan S, et al. *Phys. Rev. Lett.* 107:191804 (2011)
84. Antonello M, et al. arXiv:1503.01520 [physics.ins-det] (2015)
85. Berlin A, Gori S, Schuster P, Toro N. *Phys. Rev. D* 98:035011 (2018)
86. Abe K, et al. arXiv:1901.03750 [physics.ins-det] (2019)
87. Malbrunot C, et al. *J. Phys. Conf. Ser.* 312:102010 (2011)
88. Banerjee D, et al. *Addendum to the proposal P348: search for dark sector particles weakly coupled to muon with NA64μ*. Rep. CERN-SPSC-2018-024, CERN, Geneva. **http://cds.cern.ch/record/2640930?ln=en** (2018)
89. Gatto C. arXiv:1910.08505 [physics.ins-det] (2019)
90. McConkey N, et al. *J. Phys. Conf. Ser.* 888:012148 (2017)
91. Feng JL, Galon I, Kling F, Trojanowski S. *Phys. Rev. D* 97:035001 (2018)
92. Ball A, et al. arXiv:1607.04669 [physics.ins-det] (2016)
93. Frank M, et al. *Phys. Lett. B* 802:135204 (2020)
94. Battaglieri M, et al. arXiv:1406.3028 [physics.ins-det] (2014)
95. Balewski J, et al. arXiv:1412.4717 [physics.ins-det] (2014)
96. Arndt K, et al. arXiv:2009.11690 [physics.ins-det] (2020)
97. Andreas S, et al. *Proposal for an experiment to search for light dark matter at the SPS*. Rep. CERN-SPSC-2013-034, CERN, Geneva (2013)
98. Bauer M, Brandt O, Lee L, Ohm C. arXiv:1909.13022 [physics.ins-det] (2019)
99. Aidala CA, et al. *Nucl. Instrum. Meth. A* 930:49 (2019)
100. Banerjee D, et al. *Phys. Rev. Lett.* 118:011802 (2017)
101. Lee JP, et al. *Phys. Rev. Lett.* 119:131804 (2017)
102. Banerjee D, et al. *Phys. Rev. Lett.* 123:121801 (2019)
103. Batell B, et al. *Phys. Rev. Lett.* 113:171802 (2014)
104. Aguilar-Arevalo AA, et al. *Phys. Rev. D* 98:112004 (2018)
105. Altmannshofer W, et al. *PTEP* 12:123C01 (2019)
106. Raubenheimer T, et al. arXiv:1801.07867 [physics.acc-ph] (2018)
107. Åkesson T, et al. *Dark sector physics with a primary electron beam facility at CERN*. Rep. CERN-SPSC-2018-023, CERN, Geneva. **http://cds.cern.ch/record/2640784?ln=en** (2018)
108. deNiverville P, Pospelov M, Ritz A. *Phys. Rev. D* 92:095005 (2015)
109. Agnese R, et al. *Phys. Rev. D* 95:082002 (2017)
110. Celentano A, Darmé L, Marsicano L, Nardi E. *Phys. Rev. D* 102:075026 (2020)
111. Marsicano L, et al. *Phys. Rev. Lett.* 121:041802 (2018)
112. Fabbrichesi M, Gabrielli E, Lanfranchi G. *The Physics of the Dark Photon: A Primer*. Cham: Springer Nature Switzerland (2021)
113. Berlin A, et al. *Phys. Rev. D* 102:095011 (2020)
114. Merkel H, et al. *Phys. Rev. Lett.* 112:221802 (2014)
115. Aaij R, et al. *Phys. Rev. Lett.* 124:041801 (2020)
116. CMS Collab. *Search for a narrow resonance decaying to a pair of muons in proton-proton collisions at 13 TeV*. Rep. CMS-PAS-EXO-19-018, CERN, Geneva (2019)
117. Lees JP, et al. *Phys. Rev. Lett.* 113:201801 (2014)
118. Archilli F, et al. *Phys. Rev. Lett. B* 706:251 (2012)
119. Babusci D, et al. *Phys. Lett. B* 720:111 (2013)
120. Babusci D, et al. *Phys. Lett. B* 736:459 (2014)
121. Anastasi A, et al. *Phys. Lett. B* 757:356 (2016)
122. Batley JR, et al. *Phys. Lett. B* 746:178 (2015)
123. Marsicano L, et al. *Phys. Rev. D* 98:015031 (2018)
124. Gninenko SN. *Phys. Lett. B* 713:244 (2012)
125. Chang JH, Essig R, McDermott SD. *J. High Energy Phys.* 1701:107 (2017)
126. Ilten P, et al. *Phys. Rev. Lett.* 116:251803 (2016)
127. Ilten P, Thaler J, Williams M, Xue W. *Phys. Rev. D* 92:115017 (2015)

128. Adrian PH, et al. *Phys. Rev. D* 98:091101 (2018)
129. Doria L, et al. arXiv:1908.07921 [hep-ex] (2019)
130. Bertrand E, Essig R, Zhong YM. *J. High Energy Phys.* 1501:113 (2015)
131. Curtin D, Essig R, Gori S, Shelton J. *J. High Energy Phys.* 1502:157 (2015)
132. Vogel H, Redondo J. *J. Cosmol. Astropart. Phys.* 1402:029 (2014)
133. Chang JH, et al. *J. High Energy Phys.* 1809:51 (2018)
134. Hagley EW, Pipkin FM. *Phys. Rev. Lett.* 72:1172 (1994)
135. Badertscher A, et al. *Phys. Rev. D* 75:032005 (2007)
136. Prinz AA, et al. *Phys. Rev. Lett.* 81:1175 (1998)
137. Magill G, et al. *Phys. Rev. Lett.* 122:071801 (2019)
138. Marocco G, Sarkar S. *SciPost Phys.* 10:043 (2021)
139. Davidson S, et al. *J. High Energy Phys.* 0005:003 (2000)
140. Jaeckel J, et al. *Phys. Dark Univ.* 2:111 (2013)
141. Kovetz ED, et al. *Phys. Rev. D* 98:103529 (2018)
142. Liu H, et al. *Phys. Rev. D* 100:123011 (2019)
143. Monsalve RA, et al. *Astrophys. J.* 863:11 (2018)
144. Kelly KJ, et al. *Phys. Rev. D* 100:015043 (2019)
145. Winkler MW. *Phys. Rev. D* 99:015018 (2019)
146. Bergsma F, et al. *Phys. Lett. B* 157:458 (1985)
147. Artamonov AV, et al. *Phys. Rev. Lett.* 101:191802 (2008)
148. Cortina Gil E, et al. arXiv:2011.11329 [hep-ex] (2020)
149. MicroBooNE Collab. *Search for a Higgs Portal scalar decaying to electron-positron pairs in MicroBooNE.* MicroBooNE Note 1092-PUB, Fermilab, Batavia, IL. **https://microboone.fnal.gov/wp-content/uploads/MICROBOONE-NOTE-1092-PUB.pdf** (2020)
150. Egana-Ugrinovic D, Homiller S, Meade P. *Phys. Rev. Lett.* 124:191801 (2020)
151. Dev Bhupal, Mohapatra R, Zhang Y. *Phys. Rev. D* 101:075014 (2020)
152. Aaij R, et al. *Phys. Rev. D* 95:071101 (2017)
153. Aaij R, et al. *Phys. Rev. Lett.* 115:161802 (2015)
154. Wei JT, et al. *Phys. Rev. Lett.* 103:171801 (2009)
155. Filimonova A, Schäfer R, Westhoff S. *Phys. Rev. D* 101:095006 (2020)
156. Fradette A, Pospelov M. *Phys. Rev. D* 96:075033 (2017)
157. Krnjaic G. *Phys. Rev. D* 94:073009 (2016)
158. deNiverville P, McKee D, Ritz A. *Phys. Rev. D* 86:035022 (2012)
159. Aloni D, Soreq Y, Williams M. *Phys. Rev. Lett.* 123:031803 (2019)
160. Irastorza I, Redondo J. *Prog. Part. Nucl. Phys.* 102:89 (2018)
161. Ballou R, et al. *Phys. Rev. D* 92:092002 (2015)
162. Della Valle F, et al. *Eur. Phys. J. C* 76:24 (2016)
163. Anastassopoulos V, et al. *Nat. Phys.* 13:584 (2017)
164. Du N, et al. *Phys. Rev. Lett.* 120:151301 (2018)
165. Bähre R, et al. *J. Instrum.* 8:T09001 (2013)
166. Armengaud E, et al. *J. Instrum.* 9:T05002 (2014)
167. Silva-Feaver M, et al. *IEEE Trans. Appl. Supercond.* 27:1400204 (2017)
168. Brun P, et al. *Eur. Phys. J. C* 79:186 (2019)
169. Acciarri M, et al. *Phys. Lett. B* 345:609 (1995)
170. Abreu P, et al. *Phys. Lett. B* 268:296 (1991)
171. Abreu P, et al. *Phys. Lett. B* 327:386 (1994)
172. Acciarri M, et al. *Phys. Lett. B* 353:136 (1995)
173. Jaeckel J, Spannowsky M. *Phys. Lett. B* 753:482 (2016)
174. Abudinén F, et al. *Phys. Rev. Lett.* 125:161806 (2020)
175. Döbrich B. arXiv:1708.05776 [hep-ph] (2017)
176. Banerjee D, et al. *Phys. Rev. Lett.* 125:081801 (2020)
177. Blümlein J, et al. *Z. Phys. C* 51:341 (1991)

178. Halprin A, Andersen CM, Primakoff H. *Phys. Rev.* 152:1295 (1966)
179. Larin I, et al. *Phys. Rev. Lett.* 106:162303 (2011)
180. Aloni D, Fanelli C, Soreq Y, Williams M. *Phys. Rev. Lett.* 123:071801 (2019)
181. Knapen S, et al. *Phys. Rev. Lett.* 118:171801 (2017)
182. Sirunyan A, et al. *Phys. Lett. B* 797:134826 (2019)
183. Aad G, et al. arXiv:2008.05355 [hep-ex] (2020)
184. Aaboud M, et al. *J. High Energy Phys.* 1609:1 (2016)
185. Aad G, et al. *Eur. Phys. J. C* 76:210 (2016)
186. Bauer M, et al. *J. High Energy Phys.* 1712:44 (2017)
187. Knapen S, Lin T, Zurek KM. *Phys. Rev. D* 96:115021 (2017)
188. Dolan MJ, et al. *J. High Energy Phys.* 1712:94 (2017)
189. Drewes M, Hajer J, Klaric J, Lanfranchi G. *J. High Energy Phys.* 1807:105 (2018)
190. Caputo A, Hernández P, López-Pavón J, Salvado J. *J. High Energy Phys.* 1706:112 (2017)
191. Bernardi G, et al. *Phys. Lett. B* 203:332 (1988)
192. Vaitaitis A, et al. *Phys. Rev. Lett.* 83:4943 (1999)
193. Artamonov AV, et al. *Phys. Rev. D* 91:052001 (2015). Erratum. *Phys. Rev. D* 91:059903 (2015)
194. Aoki M, et al. *Phys. Rev. D* 84:052002 (2011)
195. Britton DI, et al. *Phys. Rev. D* 46:885 (1992)
196. Badier J, et al. *Z. Phys. C* 31:341 (1986)
197. Aguilar-Arevalo A, et al. *Phys. Rev. D* 97:072012 (2018)
198. Abe K, et al. *Phys. Rev. D* 100:052006 (2019)
199. Cortina Gil E, et al. *Phys. Lett. B* 807:135599 (2020)
200. Leventsev D, et al. *Phys. Rev. D* 87:071102 (2013). Erratum. *Phys. Rev. D* 95:099903 (2017)
201. Abreu P, et al. *Z. Phys. C* 74:57 (1997). Erratum. *Z. Phys. C* 75:580 (1997)
202. Asd G, et al. *J. High Energy Phys.* 1910:265 (2019)
203. Sirunyan AM, et al. *Phys. Rev. Lett.* 120:221801 (2018)
204. Dib CO, et al. *Phys. Rev. D* 101:093003 (2020)
205. Ballett P, Boschi T, Pascoli S. *J. High Energy Phys.* 2003:111 (2020)
206. Sabti N, Magalich A, Filimonova A. *J. Cosmol. Astropart. Phys.* 2011:056 (2020)

Annual Review of Nuclear and Particle Science

Volume 71, 2021

Contents

Errata

An online log of corrections to *Annual Review of Nuclear and Particle Science* articles may be found at http://www.annualreviews.org/errata/nucl